## ABSTRACT

## COATING OF ALUMINUM POWDER WITH POLYMERS IN SUPERCRITICAL CARBON DIOXIDE

**by**
**Li Yuan**

Eleven polymers were used to produce coatings (2-20 nm) on the surface of an aluminum powder to modify its properties. The polymers studied are polyisobutylene (PIB), poly (vinylidene fluoride) (PVF), poly (methyl methacrylate) (PMMA), polystyrene (PS), poly(ethylene terephthalate) (PETP), poly(4-vinylbiphenyl) (PVB), poly(4-vinylpyridine) (PVP), poly(4-bromostyrene) (PBS), poly (vinylidene fluoride-*co*-hexafluoropropylene) (PVFH), poly (styrene-*co*-methyl methacrylate) (PSMMA), poly (vinyl chloride-*co*-vinyl acetate) (PVCVA). Supercritical carbon dioxide was used as a solvent and as a transport medium. Coated aluminum powders exhibit enhanced resistance to the dissolution in basic solutions. The protective properties of the polymeric films were quantified based on the dissolution rate. Polymeric films that contain aromatic rings were characterized using UV absorption spectrophotometry. Temperature and pressure were varied over 84 – 210 °C and 80 – 480 atm to determine the optimal condition for coating. A technique to measure the solubilities of poorly soluble polymers in supercritical carbon dioxide was developed. The solubility of PVB is determined as 11.7 mg/L at T = 170 °C and p = 341 atm. The study of the morphology of the coated powder was carried on by using an Environmental Scanning Electron Microscope (ESEM) and an Electron-Dispersive X-ray Detector (EDX). The coatings produced using supercritical carbon dioxide as well as using organic solvents were compared and evaluated.

# COATING OF ALUMINUM POWDER WITH POLYMERS IN SUPERCRITICAL CARBON DIOXIDE

by
Li Yuan

A Thesis
Submitted to the Faculty of
New Jersey Institute of Technology
In Partial Fulfillment of the Requirements for the Degree of
Master of Science in Applied Chemistry

Department of Chemical Engineering, Chemistry and Environmental Science

May 2001

**APPROVAL PAGE**

# COATING OF ALUMINUM POWDER WITH POLYMERS IN SUPERCRITICAL CARBON DIOXIDE

**Li Yuan**

---

Dr. Lev N. Krasnoperov, Thesis Advisor — Date
Professor of Chemistry, NJIT

---

Dr. Joseph Bozzelli, Committee Member — Date
Distinguished Professor of Chemistry , NJIT

---

Dr. Robert Pfeffer, Committee Member — Date
Distinguished Professor of Chemical Engineering, NJIT

## BIOGRAPHICAL SKETCH

**Author**: Li Yuan

**Degree**: Master of Science

**Date**: May 2001

**Undergraduate and Graduate Education:**

Master of Science in Applied Chemistry
New Jersey Institute of Technology, Newark, NJ, 2001

Bachelor of Science in Analytical Chemistry,
Sichuan University, Sichuan, P. R. China, 1999

**Major:** Applied Chemistry

**Presentations**

Li Yuan,
"Coating of Al Powder with Polymers in Supercritical Carbon Dioxide",
The Ninth Annual Uni-Tech Student Conference on Science and Technology,
New Jersey, USA, April 2000.

To my beloved family

## ACKNOWLEDGMENT

I would like to express my deepest appreciation to Professor Lev. N. Krasnoperov, who not only served as my research advisor, providing valuable and countless resources, insight, and intuition, but also constantly gave me support, encouragement, and reassurance. Special thanks are given to Dr. Joseph Bozzelli and Dr. Robert Pfeffer for actively participating in my committee.

I would like to thank Department of Chemical Engineering, Chemistry and Environmental Science and the US Army Sustainable Green Manufacturing Program for the financial support.

I would also thank Dr. Evgeni Glebov and Dr. Oleg Usov for their help over the years.

## TABLE OF CONTENTS

## TABLE OF CONTENTS
## (Continued)

## LIST OF TABLES

## LIST OF FIGURES

## LIST OF FIGURES
## (Continued)

**Figure** **Page**

## LIST OF FIGURES
## (Continued)

**Figure** **Page**

## LIST OF FIGURES
## (Continued)

**Figure** **Page**

# CHAPTER 1

# INTRODUCTION

## 1.1 What Is Supercritical Fluid?

Supercritical fluid is a state of a substance when temperature and pressure are above its critical temperature and pressure (critical point). The critical temperature of a substance is the temperature above which liquid phase can not exist, regardless of pressure. The vapor pressure of a substance at its critical temperature is its critical pressure. Supercritical fluids are attractive in many applications because of their unique properties. Near the critical point, the molar volume or density of a substance changes dramatically with pressure. Supercritical fluids exhibit liquid-like densities and increased solvent power near the critical region. In addition, their gas-like viscosities and high diffusivities are beneficial for mass transfer. These unique solubility properties allow some compounds which are insoluble in a fluid at ambient conditions to become soluble in supercritical conditions. The density, solvating power, transport and other properties of supercritical fluids can be adjusted by altering pressure and temperature (Rindfleisch *et al.*, 1996; Kim and Johnston, 1987; Savage *et al.*, 1995).

## 1.2 The Development of the Application of Supercritical Carbon Dioxide

About 25 years ago, low-pressure catalysis was dominated in industrial applications such as production of polyethylene and ammonia industries. High-pressure research seemed not to have any significant commercial interest. There has been limited research devoted to high - pressure industrial applications (Teja and Eckert, 2000).

However, immediately after the first session on supercritical fluids held on AIChE meeting (New Orleans, 1980), the industrial potential of supercritical fluids was realized. Since then, a number of universities and industrial laboratories began research in this area.

At the beginning, most of the applications were still limited to fossil fuel processing and food processing. However, during the past two decades, supercritical technologies have been developing very rapidly. Since the middle of 1980s, supercritical fluids were explored for other fast growing areas such as extraction, purification, solvent replacement, green chemistry, particle production, material processing, analytical application, etc (Teja and Eckert, 2000; Perrut, 2000). In recent years, a significant amount of research on supercritical fluids has been devoted to alternative solvents as an environmental benign substitute for hydrocarbons and chloroflurocarbons (Engelhardt and Jurs, 1997). The use of $CO_2$ as a solvent instead of traditional organic solvents has attracted much attention.

Carbon dioxide has a number of advantages:

(1) Carbon dioxide has modest critical parameters, such as low critical temperature ($T_c$ = 304.2 K) and a moderate critical pressure ($p_c$ = 72.8 atm).

(2) carbon dioxide is non-toxic, non-corrosive and very inexpensive (less than $ 0.2/kg).

(3) Third, carbon dioxide has a higher density than most other SCF, which means that at temperatures slightly above ambient it is possible to obtain liquid-like densities and liquid-like solvent characteristics (Cooper, 2000; Cooper and DeSimone, 1996). The phase diagram of carbon dioxide is shown in Figure 1.

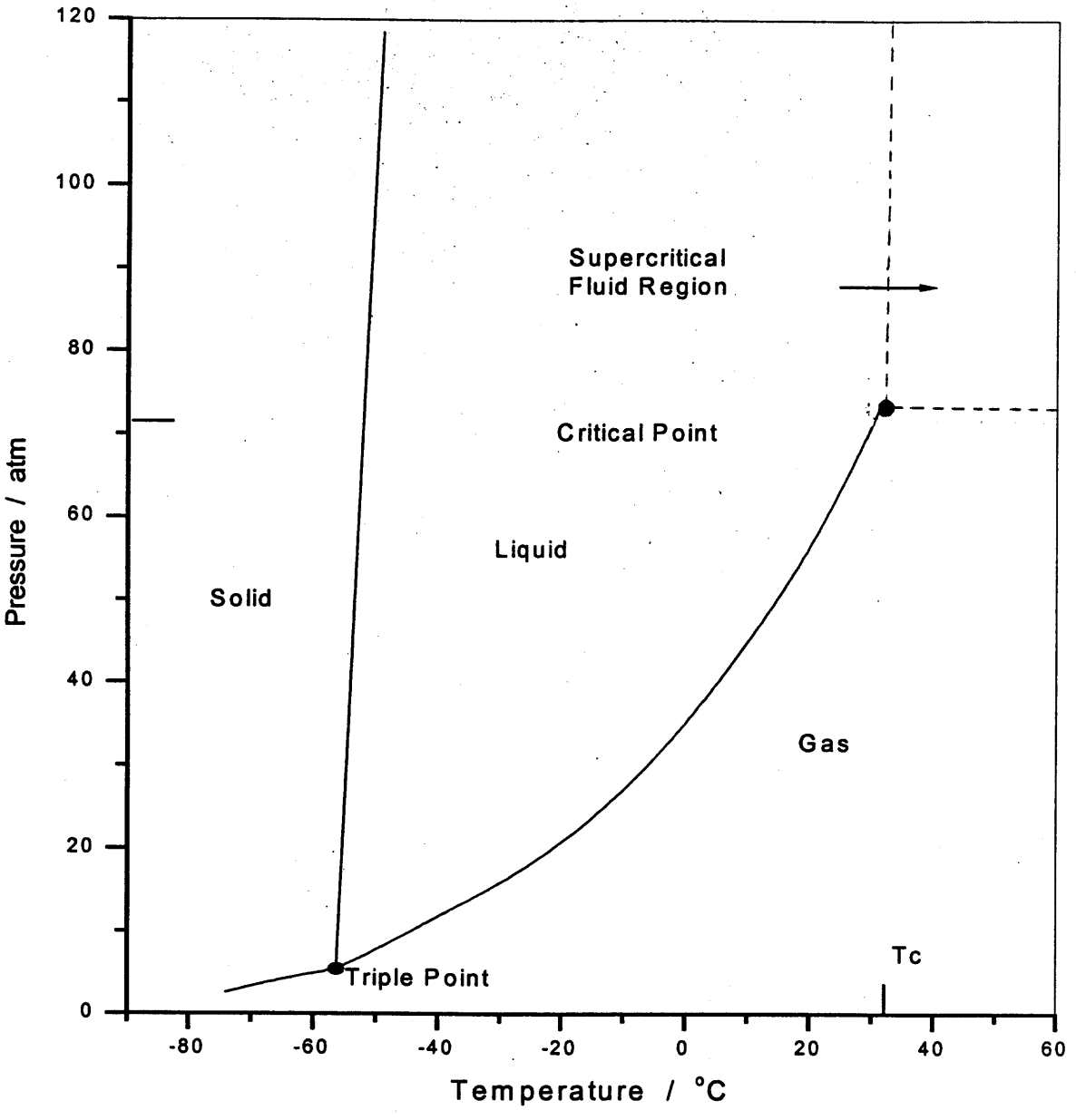


**Figure 1.2** Phase diagram of carbon dioxide (McHugh and Krukonis, 1986).

Supercritical carbon dioxide has been widely used in industry as a prospective medium for a number of chemical engineering processes (Ikushima and Saito, 1992). The application of supercritical carbon dioxide for production of fine particles is

based on the strong effect of pressure on the solubilities of low-volatile compounds in supercritical carbon dioxide. Formation of solid particles upon decompression of supercritical carbon dioxide solution was first observed more than one hundred years ago (Hannay and Hogarth, 1879). More recently, the formation of fine particles during the expansion of solutions in supercritical carbon dioxide through a valve was observed for a number of different solutes (Paulaitis *et al.*, 1983; McHuge *et al.*, 1986; Larson and King, 1986; Ma and Tomasko, 1986). Further development of this approach is rapid expansion of supercritical solution (RESS) technique (Petersen *et al.*, 1986; Matson *et al.*, 1987; Mohamed *et al.*, 1989; Chang *et al.*, 1989; Tom *et al.*, 1991), in which a supercritical solution is expanded across a fine throttling device.

### 1.3 Coating of Particles

The objective of coating is to deposit coating materials on the surface of particles or substrates to modify their properties such as appearance, color, flavor, resistance to environment, etc. It has been widely employed in various industries, including paint industry, pyrotechnics formulations and pharmaceutical field for the manufacturing of new drug delivery systems to delay drug release (Noriyuki *et al.*, 1998; Re and Biscans, 1999).

Metals and alloys have tremendous use in a great variety of practical applications. However, most metals are active and can be corroded, especially in harsh environments such as high temperatures, humidity, oxidative environments, etc, or their combinations. The corrosion of metals is a multi-billion dollar world-wide problem that results in the loss of the material, energy, even life. By coating of metal

parts and other objects made of metals, their resistance to the environments can be significantly improved. Passive films coated on metal surfaces act as physical barriers between the metal surface and the corrosive environment, thus protecting it from humidity, oxygen, alkali or acids, etc.

There are three types of materials: inorganic, organic and metallic materials that can be used as the coating materials, depending on the purpose of the coating. Polymer coatings have received significant attention during recent years. This project is devoted to production and investigation of polymer coatings on metal powders. Coatings of metal powders are used in pyrotechnic and rocket fuel techniques since it can reduce their deterioration through corrosion and aggregation caused by moisture or other aggressive surroundings. In this study, eleven polymers were used for coating of Al powder using supercritical carbon dioxide as a solvent.

## 1.4 Objectives of the Research

The objectives of this research were:

1) to produce various polymeric films on the surface of Al powder in supercritical carbon dioxide,
2) to characterize the protective properties of the polymeric films both qualitatively and quantitatively,
3) to characterize the polymeric film thickness produced under different deposition conditions,
4) to determine the optimal condition for coating Al powder with polymers in supercritical carbon dioxide,

5) to characterize the morphology of the coated aluminum powders ,

6) to compare the coating properties for samples coated from SC $CO_2$ and from common organic solvents.

To achieve the objectives, a number of polymers (11) were used as coating materials. The protective properties of the polymeric films were evaluated by measuring the dissolution rate of the coated Al powders in NaOH solution. UV spectrophotometry was employed to measure the film thickness. The working temperature, deposition pressure and discharge temperature were varied to determine the optimal condition. The morphology of the coated Al powders was studied using an environmental scanning electron microscope (ESEM) and an electron dispersive X-ray (EDX) detector. The results were compared with that obtained for Al powder coated in common organic solvent.

# CHAPTER 2

# EXPERIMENTAL SECTION

## 2.1 Coating of Aluminum Powders with Polymers from SC $CO_2$ and Common Organic Solvents

For coating of aluminum powders in SC $CO_2$, a batch stirred high-pressure temperature controlled reactor (Autoclave Engineers, BC 0030 SS 05AH, 300 $cm^3$ volume) was used. The experimental set-up is shown in Figure 2.1.

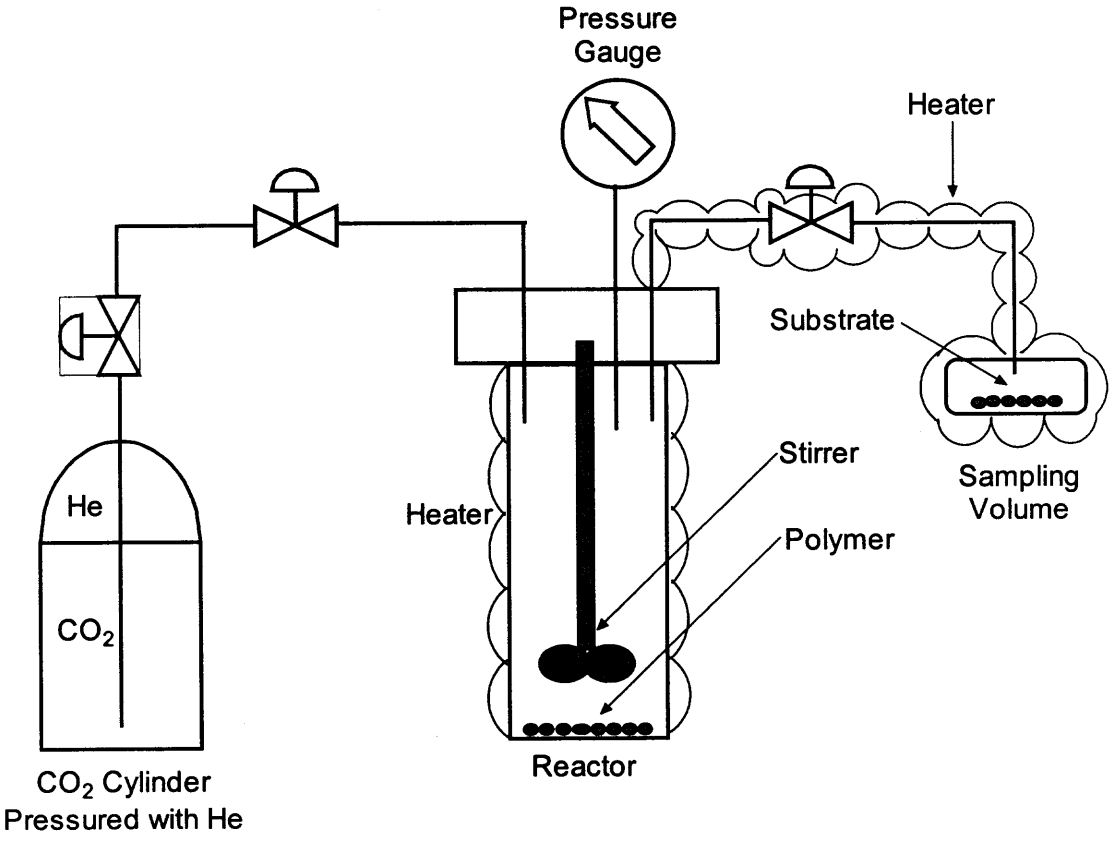


**Figure 2.1** Sketch of the stirred high pressure-temperature batch reactor.

Weighed amounts of polymers — powders or chips (200 mg in this study) were loaded into the reactor and a sample of Al powder was placed into an auxiliary volume (ca. 5 $cm^3$) connected to the reactor. Polymers and aluminum powders used in this study are presented in section 2.5. The whole coating system was cleaned with ca. 1.1 atm pressure of $CO_2$ to remove air. Then the reactor was disconnected from the sample volume and filled with a 98% fraction of the targeted amount of carbon dioxide, with pressure about 100 atm. The experimental conditions were varied through the variation of the initial pressure and temperature.

After loading $CO_2$, all the valves in the system were closed and the reactor was heated to a working temperature (80 to 250 °C) using an oven. Temperature was increased slowly in order to prevent overheating. The mixture of polymer and SC $CO_2$ in the reactor was stirred by a magnetic drive stirrer with a constant rate (ca. 1 revolution per second). The heating and temperature of the sampling volume were controlled independently of the reactor temperature.

After achieving the working temperature of the reactor and the sample volume, temperature was kept constant. The stirring was stopped and the whole reaction system was allowed to relax. After ca. 10 minutes, the sampling vent was open to allow the SC $CO_2$ into the sample volume. After ca. 5 minutes, the sampling volume was closed again and allowed to cool down. The sampling volume was discharged at 40 -120 °C through the empty reactor. Then the sampling volume was disconnected from the reactor and the coated Al powder was collected and analyzed. To compare the properties of the samples coated from supercritical $CO_2$ and from the

common organic solution, aluminum powders were also coated using a common solvent (dichloromethane). Solutions of polymers with known mole fractions of monomer units of polymers were prepared by the following procedure. Pre-calculated amounts of polymers were dissolved in dichloromethane ($CH_2Cl_2$), after which weighed amounts of metal powder were placed in polymer solutions. The polymers were deposited on the surface of Al powder by evaporation of the solvent. The chemical structures and physical properties of the polymers used in this study are listed in Table 2.11 and 2.12.

**Table 2.11** Chemical Structures of Polymers Used in This Study

| Polymer | Chemical Formula of Monomer | Structure of Monomer Unit |
|---|---|---|
| PIB (Polyisobutylene) | $C_4H_8$ | $-CH_2-C(CH_3)_2-$ |
| PVF (Poly(vinylidene fluoride)) | $C_2H_2F_2$ | $-CH_2CF_2-$ |
| PMMA (Poly(methyl methacrylate)) | $C_5H_8O_2$ | $-CH_2C(CH_3)(CO_2CH_3)-$ |
| PS (Polystyrene) | $C_8H_8$ | $-CH_2CH(C_6H_5)-$ |
| PETP (Poly(ethylene terephthalate)) | $C_{10}H_8O_4$ | $-OCH_2CH_2O_2CC_6H_4-4-CO-$ |
| PVB (Poly(4-vinylbiphenyl)) | $C_{14}H_{12}$ | $-CH_2CH(C_6H_4C_6H_5)-$ |
| PBS (Poly(4-bromostyrene)) | $C_8H_7Br$ | $-CH_2CH(C_6H_4Br)-$ |
| PVP (Poly(4-vinylpyridine)) | $C_7H_7N$ | $-CH_2CH(C_5H_4N)-$ |
| PVFH (Poly(vinylidene fluoride-*co*-hexafluoropropylene)) | $x[C_2H_2F_2]$ $y[C_3F_6]$ | $[-CH_2CF_2-]_x$ $[CF_2CF(CF_3)-]_y$ |
| PSMMA (Poly(styrene-*co*-methyl methacrylate)) | $0.6[C_5H_7O_2]_y$ $+0.4[C_8H_8]_x$ | $[-CH_2CH(C_6H_5)-]_x$ $[-CH_2C(CH_3)(CO_2CH_3)]_y$ |
| PVCVA (Poly(vinyl chloride – *co* - vinyl acetate)) | $[C_2H_3Cl]_x$ $+[C_4H_6O_2]_y$, 86 wt.% vinyl chloride | $[-CH_2CHCl-]_x$ $[-CH_2C(CH_3)(CO_2CH_3)-]_y$ |

**Table 2.12** Physical Properties of Polymers Used in This Study

| Polymer | Formula of monomer | M/gmol$^{-1}$ [1] | D/gcm$^{-3}$ [2] | $t_m$/°C [3] | $t_g$/°C [4] | $\delta$ / MPa$^{1/2}$ [5] | $E_{coh}$/kJmol$^{-1}$ [6] |
|---|---|---|---|---|---|---|---|
| PIB | $C_4H_8$ | 56 | 0.92 | 1.5 | | 15.4– 15.8 | 14.6 – 15.9 |
| PVF | $C_2H_2F_2$ | 45 | 1.78 | 166-170 | -38 | 23.2 | 13.2 – 13.6 |
| PMMA | $C_5H_8O_2$ | 100 | 1.19 | | 114 | 18.3– 22.7 | 29.9 – 43.3 |
| PS | $C_8H_8$ | 104 | 1.047 | 240 | 100 | 17.5– 18.6 | 30.4 – 34.3 |
| PETP | $C_{10}H_8O_4$ | 192 | 1.375 | 270-310 | 81 | 21.9 | 66.9 |
| PVB | $C_{14}H_{12}$ | 180 | | | 138 | | |
| PBS | $C_8H_7Br$ | 183 | | | | | |
| PVP | $C_7H_7N$ | 110 | | | 142 | | |
| PVFH | x[$C_2H_2F_2$] y[$C_3F_6$] | Ca. 107 | 1.77 | 140-145 | | | |
| PSMMA | 0.6[$C_5H_7O_2$]$_y$ + 0.4[$C_8H_8$]$_x$ | 108.8 | | | 101 | | 34.8[7] |
| PVCVA | [$C_2H_3Cl$]$_x$ + [$C_4H_6O_2$]$_y$, 86 wt.% vinyl chloride. | 65 | | | 72 | | 17.9[7] |

[1]Molar mass of monomer
[2]Density
[3]Melting point
[4]Glass transition temperature
[5]Solubility parameter
[6]Cohesive energy
[7] where $E_{coh}^{(1,2)} = \Sigma x_i E_{coh}^{(i)}$, is the cohesive energy for co-polymer, $E_{coh}^{(i)}$, i = 1,2, are the cohesive energies for pure polymers, and $x_i$ is a mole fraction of polymer (i) in the composition of co-polymer.

## 2.2 Analysis of Samples Using UV Spectrophotometry

To characterize the efficiency of the polymer deposition, the film thickness of the polymers deposited on the surface of Al powder particles was measured. For this purpose, UV absorption spectra were employed. Several polymers used in the current study contain aromatic groups (such as PVB, PVP, etc) and have strong absorption in the near UV region, which allows convenient and sensitive qualitative and quantitative characterization of the polymer film thickness.

First, the mole absorptivity, $\varepsilon_{poly}$, was determined using the following procedure. At least 4 different concentration of the polymer solutions were prepared and measured using a UV spectrophotometer. Varian DMS 300 UV-Vis spectrophotometer was used to record the UV absorption spectra. Examples of polymer UV absorption spectra obtained in this way are shown in Figure 2.21.

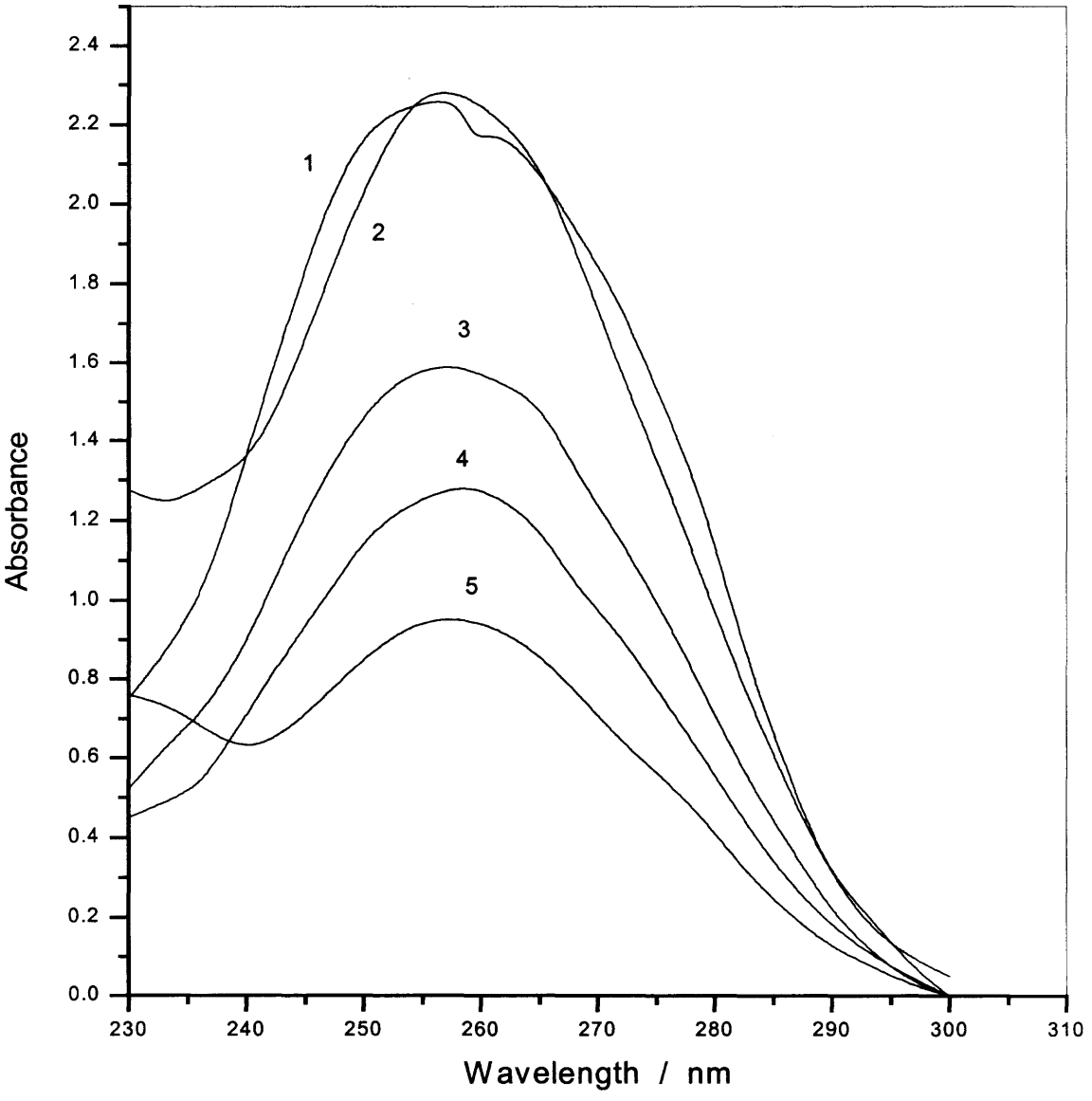


**Figure 2.21** UV absorption spectra of PVP. 1. Standard poly (4 - vinyl biphenyl), 1.5 x $10^{-4}$ M. 2. Poly (4-vinyl biphenyl) solution extracted from Al powders coated in SC $CO_2$ at 250 °C. 3. Standard poly (4-vinyl biphenyl) solution, 1x$10^{-4}$ M. 4. Poly (4-vinyl biphenyl) solution extracted from Al powders coated in SC $CO_2$ at 220 °C. 5. Poly (4 - vinyl biphenyl) solution extracted from Al powders coated in SC $CO_2$ at 200 °C.

The spectra of PVB washed from Al powder coated in SC $CO_2$ are shown together with the spectrum of standard solution. The two spectra are almost identical in shape. This indicates that no substantial polymer structure modification occurred during the coating procedure. The molar absorptivity is calculated using equation 1.

$$A = \varepsilon_{poly} l C \quad (1)$$

In this expression, $A$ is the measured absorbance, $C$ is the molar concentration of the monomer unit in the polymer solution (mol $L^{-1}$), $l$ is the thickness of the cuvette (cm), $\varepsilon_{poly}$ is the molar absorptivity of the polymer in terms of the concentration of the monomer units (L $mol^{-1}$ $cm^{-1}$).

After the molar absorptivity was obtained, the thickness of the film deposited on the powder surface was determined as follow. Weighed amounts of coated Al powders were washed with measured volumes of dichloromethane. Then the solutions were filtered through a filter paper and collected for analysis. By measuring the absorbance of these solutions, the film thickness of the polymers on the powders were calculated using equation 2:

$$h = \frac{M_{mono} A V_{solv}}{\varepsilon_{poly} l m_s S_m \rho_{poly}} \quad (2)$$

In equation 2, $M_{mono}$ is the molar mass of the monomer unit of the polymer, $A$ is the measured absorbance of the polymer solution (base 10), $V_{solv}$ is the volume of solvent used to extract polymer from the coated sample, $\varepsilon_{mono}$ is the molar absorptivity of the polymer per monomer unit , $l$ is the length of the absorption cell, $m_S$ is the mass of the coated samples, $S_m$ is the surface of a substrate particles per unit mass of the powder (1110 $cm^2/g$ for 20 $\mu$m in diameter spherical aluminum particles), and $\rho_{poly}$ is the density of the polymer of interest. Equation 2 is derived assuming spherical shape of the powder particles. The UV spectra of PBS, PVB and PVP extracted from the coated Al powders which were coated in supercritical carbon dioxide are shown in Figures 2.22, 2.23 and 2.24, respectively.

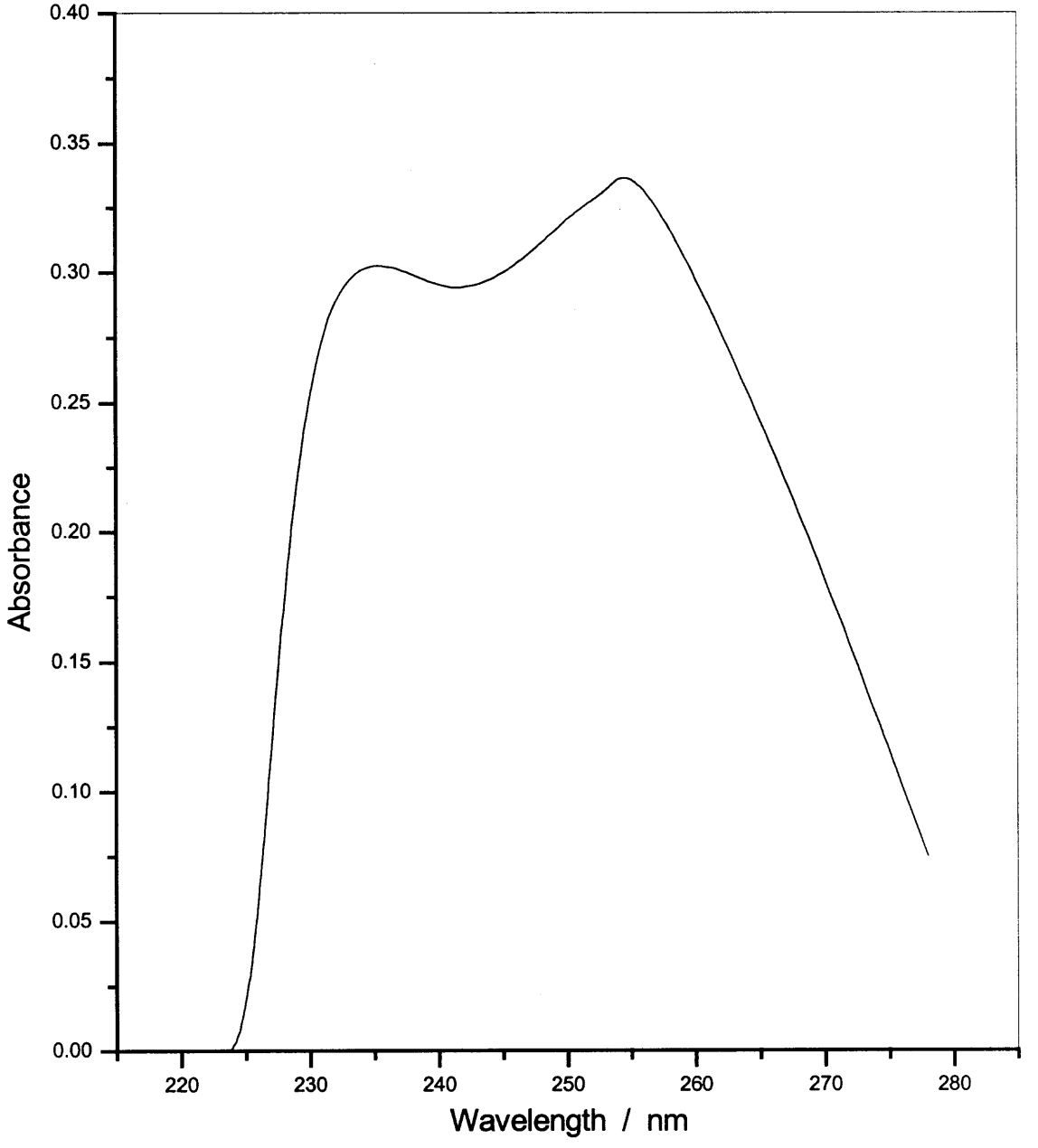


**Figure 2.22** UV absorption spectrum of PBS (solvent $CH_2Cl_2$). PBS was extracted with 2.6 ml $CH_2Cl_2$ from 72.4 mg of coated Al powders which were coated in SC $CO_2$ at 170 °C and 4000 psig.

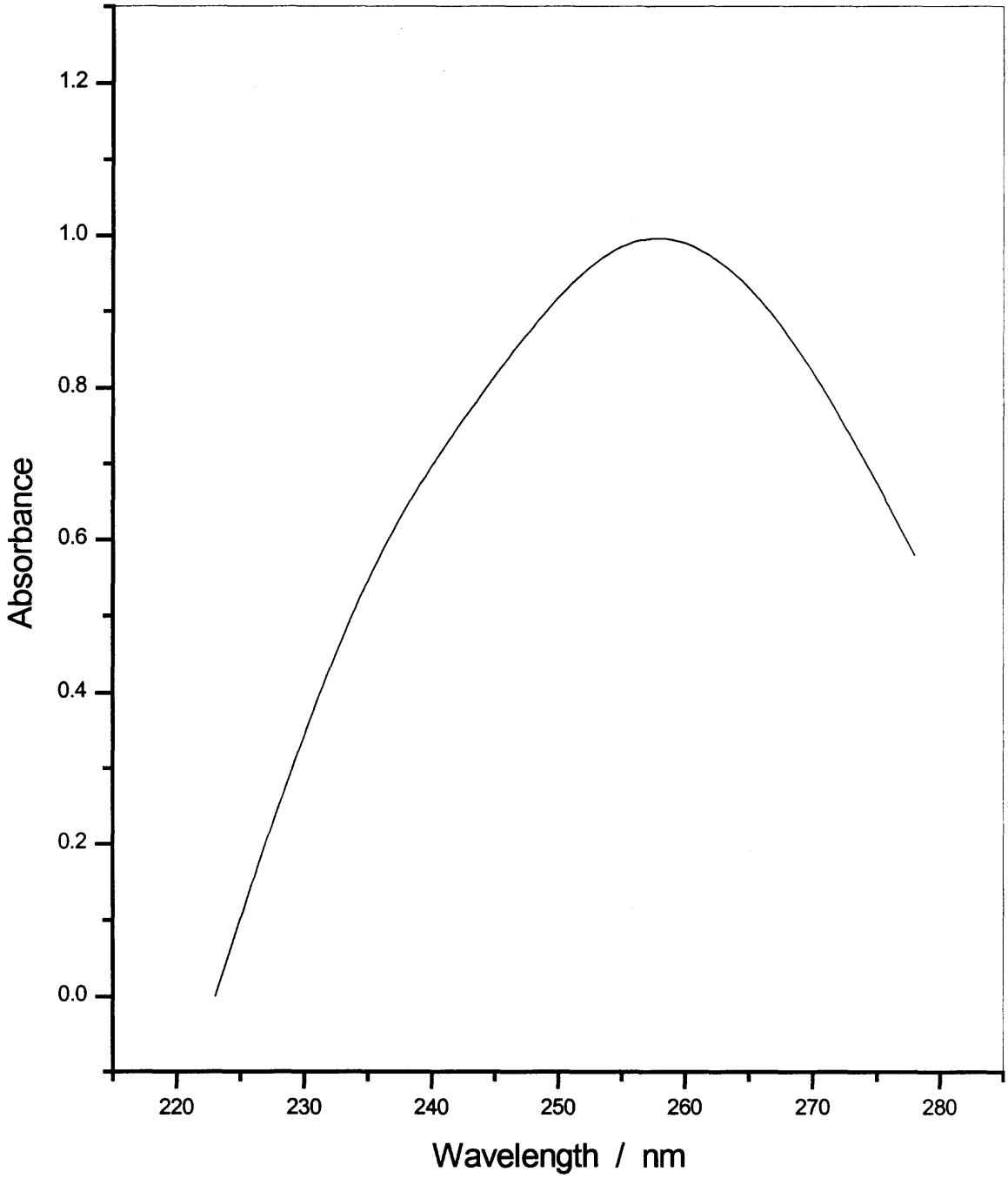


**Figure 2.23** UV absorption spectrum of PVB (solvent $CH_2Cl_2$). PVB was extracted with 2.2 ml $CH_2Cl_2$ from 74.8 mg of coated Al powders which were coated in SC $CO_2$ at 170 $^{o}$C and 4000 psig.

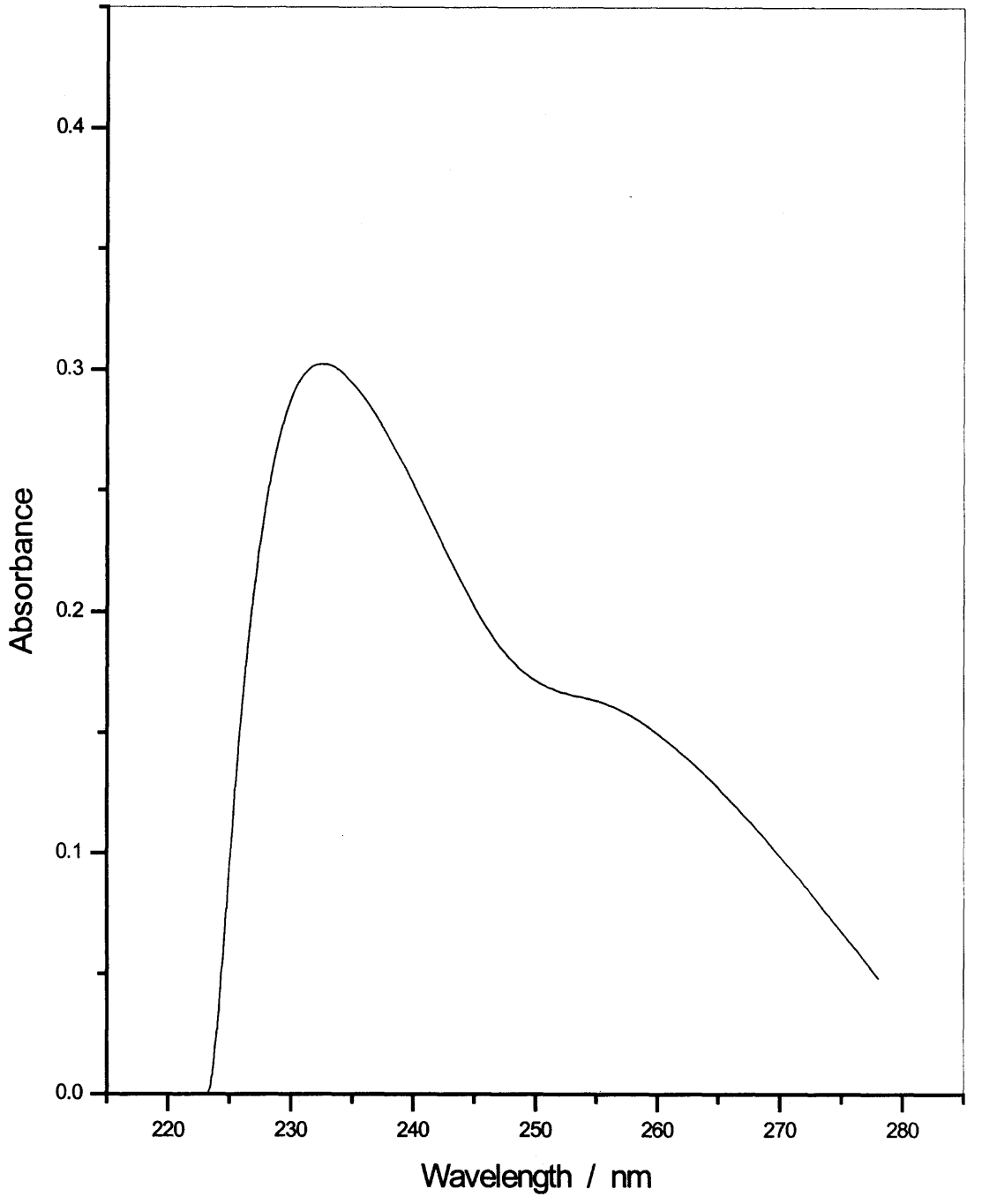


**Figure 2.24** UV absorption spectrum of PVP (solvent $CH_2Cl_2$). PVP was extracted with 2.2 ml $CH_2Cl_2$ from 89 mg of coated Al powders which were coated in SC $CO_2$ at 170 °C and 4000 psig.

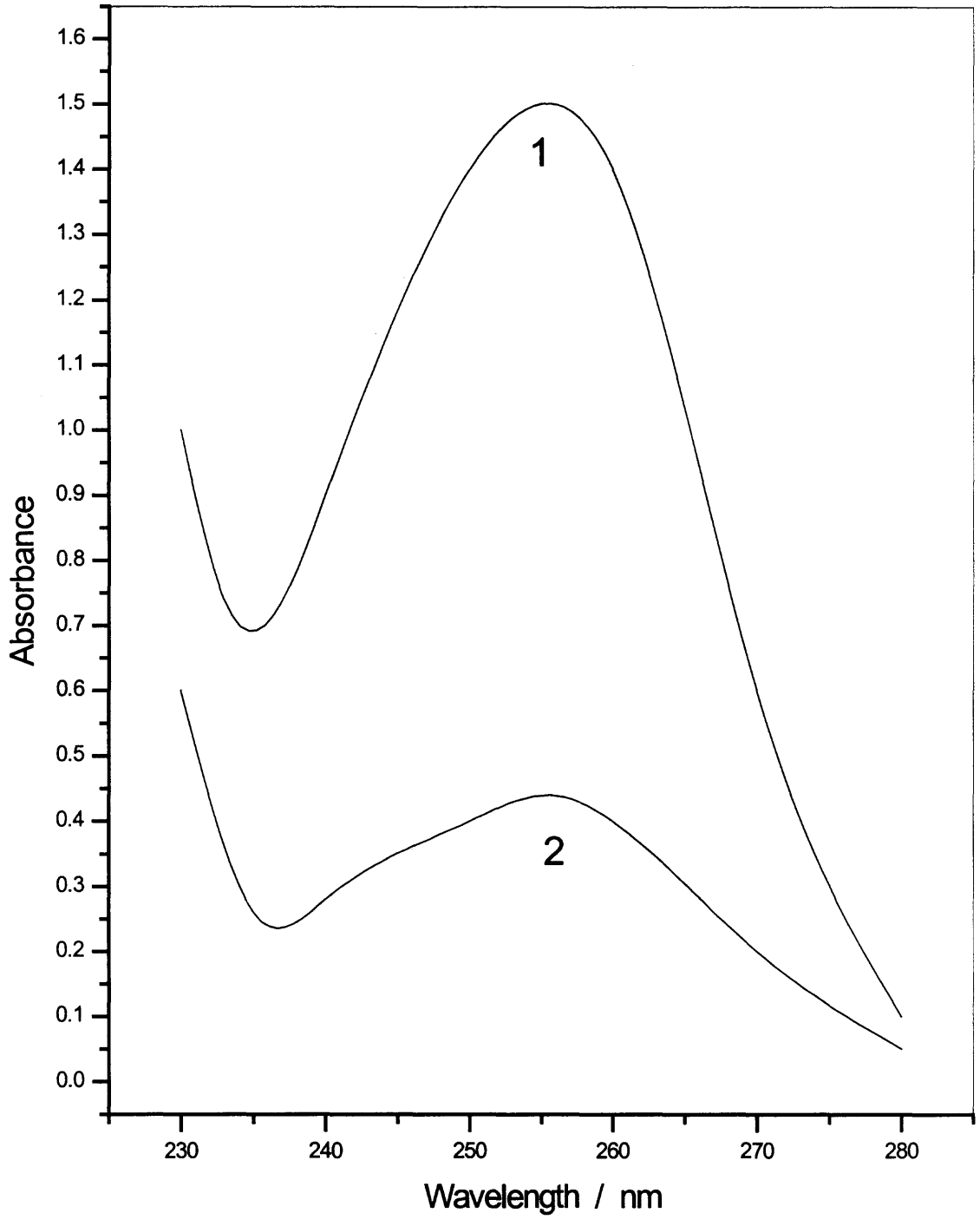


**Figure 2.25** UV absorption spectra of PVP solution extracted from Al powders coated with PVP in $CH_2Cl_2$. Curve 1 - spectrum of sample with targeted film thickness 100 nm. Curve 2 - spectrum of sample with targeted film thickness 40 nm.

By using the method described above, the maximum molar absorptivities were determined to be $\varepsilon_{poly,max}$ = 7400, 15600 and 1600 L $mol^{-1}$ $cm^{-1}$ for PBS, PVB and PVP, respectively. The wavelengths, the molar absorptivities and the film thickness for all polymers extracted from the coated aluminum powders are listed in Table 2.2.

**Table 2.2** Maximum Molar Absorptivities of Polymers per Monomer Concentration in $CH_2Cl_2$ Solutions and Thickness of the Polymers Deposited on the Surface of Al Powders from SC $CO_2$ at 170 °C, 4000 psig.

| # | Polymers | λ / nm | ε / $M^{-1}$ $cm^{-1}$ | Sample # | Thickness / nm |
|---|---|---|---|---|---|
| 1 | PVP | 256 | 1600 | 081800 | 6.2 |
| 2 | PVB | 255 | 15600 | 082100 | 3.2 |
| 3 | PBS | 230 | 7400 | 082100 | 2.7 |
| 4 | PS | 260 | 230 | 090700 | 22 |
| 5 | PSMMA | 260 | 70 | 092100 | 80 |

To illustrate the reliability of the film thickness measurements and the quantitative film deposition methods developed in this study, a series of experiments was carried on. First, samples with targeted film thickness were prepared by coating of aluminum powders from organic solutions with a calculated polymer concentration. Then the actual film thickness was measured using UV spectroscopy. Figure 7 shows the UV spectra of PVP extracted from a sample coated from an organic solvent ($CH_2Cl_2$). Spectrum 1 is the spectrum of PVP obtained from a coated aluminum sample with a targeted film thickness

of 100 nm. Spectrum 2 is the spectrum of PVP obtained from aluminum powders coated with a targeted film thickness of 40 nm. By using the information provided in this figure, the thickness was calculated to be 97.4 and 42.7 nm -- which are very close to the targeted values of 100 nm and 40 nm, respectively. The results indicate that the film thickness measurements and the quantitative film deposition methods developed in this study are reliable.

## 2.3 Characterization of the Protective Properties of Polymeric Films by Dissolution Rate in Alkali

Aluminum is a very reactive element. It can react with acids, alkali, water, but the surface of Al has a thin film of aluminum oxide film which protects the bulk aluminum from the environment. If this thin film is dissolved by a strong reagent like NaOH, the sample can be dissolved in a few minutes. Aluminum reacts with alkali solutions with the formation of molecular hydrogen (Tikhonov, 1973; Angus *et al.*, 1976).

$$Al + NaOH + H_2O \longrightarrow NaAlO_2 + 3/2\ H_2 \qquad (3)$$

Polymer films deposited on the surface of aluminum powder particles decelerate the rate of aluminum dissolution (reaction 3). The "rate constant" of dissolution of Al powders in stoichiometric quantities of 0.01 M NaOH solutions was chosen as a quantitative criterion of the protective properties of the films.

The dissolution reaction 3 was monitored via the mass loss of the powder samples. Proper account was made for the subsequent transformations of the aluminate ion, $AlO_2^-$. In aqueous solutions this ion is transformed to the $Al(OH)_4^-$ complex which is

further hydrolyzed forming insoluble aluminum hydroxide, $Al(OH)_3$ (Durrant *et* al., 1962). Aluminum hydroxide forms colloid suspension in the bulk of the solution. To avoid possible errors in the measuring the mass of the residual aluminum, the aluminum hydroxide was removed by a syringe immediately after precipitation.

The rate of dissolution of coated Al powder in NaOH solutions is a measure of the protection properties of the films. The longer the time needed for dissolution, the more resistant is the coated particle to alkali solutions. In the measurements the following procedure was used. Typically, four to five identical samples of 10.8 mg ($4.00\times10^{-4}$ moles of Al) of Al powder were placed in beakers each containing 40 mL of 0.01 M NaOH solution ($4.00\times10^{-4}$ moles of NaOH). The powders were allowed to dissolve for different periods of time, after which the process of dissolution was terminated by discharging the alkali solutions from the beakers. The powders were washed twice with water to remove aluminum hydroxide and the residual alkali solutions. Then the beakers with the residual powder were dried and weighed with and without the residual dry powder to determine the mass of the residual aluminum. Usually, four to five experimental points were obtained. The residual mass of the sample was plotted vs. the dissolution time. The experimental kinetic curves were fitted using the "second order kinetic law":

$$m_t = \frac{m_0}{1 + k\,t} \qquad (4)$$

where $m_t$ is the mass of the powder at time t, $m_0$ is the initial mass, and $k$ is the apparent rate constant. There is no fundamental justification for equation 4. It was empirically found that the experimental data could be satisfactorily fitted by equation 4.

It was observed, however, that the above procedure results in lower masses of aluminum than the loaded amounts even at zero dissolution times due to the sample loss in the washing procedure. The sample losses are caused by both the removal of a fraction of the aluminum powder with the wash water and the slow dissolution of aluminum in pure water. The loss in the sample mass is proportional to the loaded amount and was ca. 15% for uncoated and ca. 7% for coated aluminum samples per wash. After discharging the initial solution (which leads to comparable sample losses), the washing procedure was applied twice. To account for the sample losses, calibration of the dissolution experiments was performed by measuring the sample loss with zero dissolution time. The calibration for the dissolution of the uncoated aluminum powder is shown in Figure 2.31.

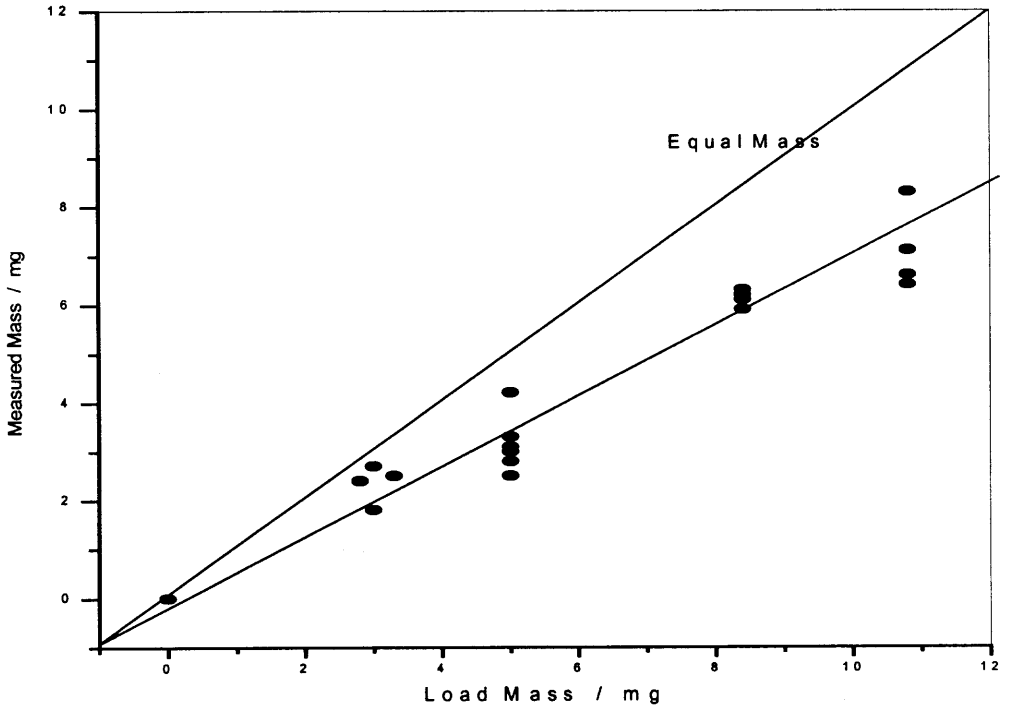


**Figure 2.31** The calibration curves for the uncoated aluminum powder in the dissolution measurements.

In the processing the experimental kinetic curves, the mass of the residual aluminum was multiplied by a correction factor to account for the sample losses. Based on Figure 2.31 the correction factor for the dissolution of uncoated aluminum powder was determined as 1.47. Similarly, the correction factor for coated powders was determined as 1.21.

The measurements of the dissolution rates were performed both with and without forced stirring of the reacting mixture. Figures 2.32 and 2.33 show the impact of stirring on dissolution of a uncoated Al powder and coated Al powder, respectively.

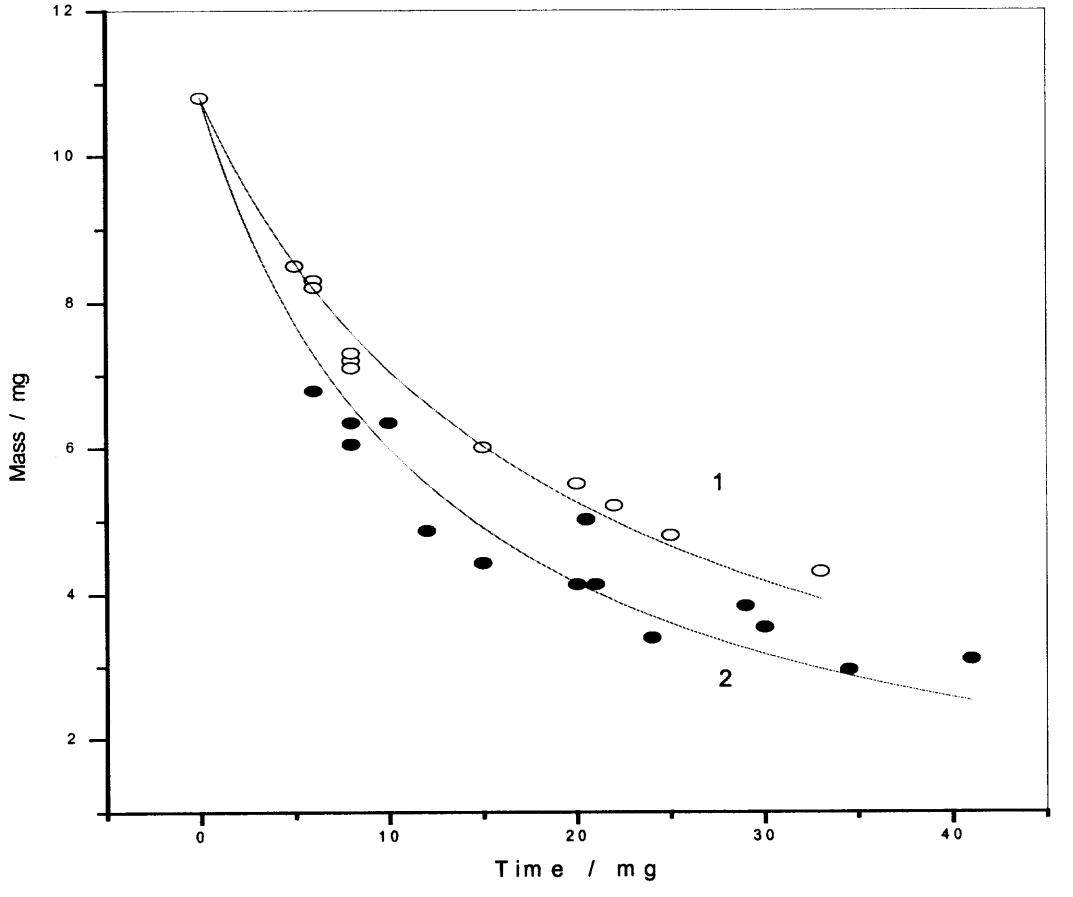


**Figure 2.32** Impact of stirring on the dissolution rate of blank Al powders.1: Without stirring, k = 0.053 $min^{-1}$. 2. With stirring, k = 0.080 $min^{-1}$.

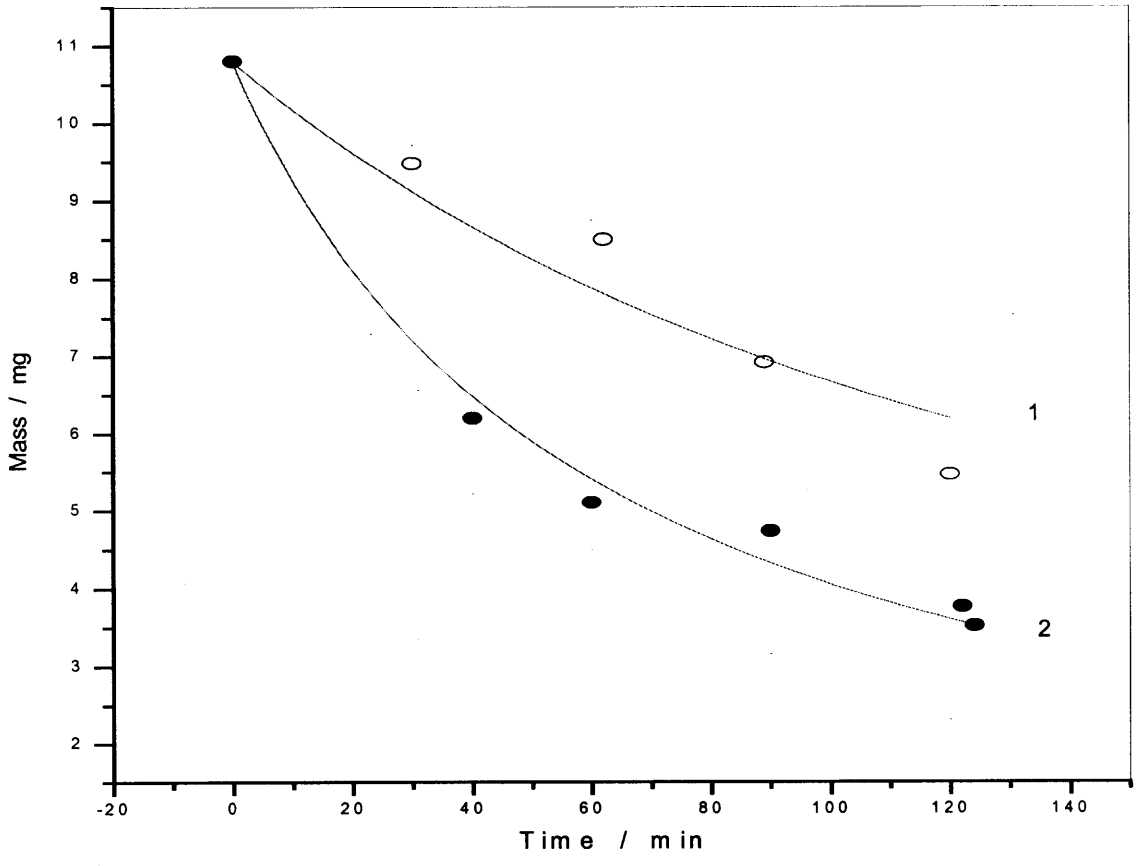


**Figure 2.33** Impact of stirring on the dissolution of samples coated with PVP in SC $CO_2$ at 170 °C and 4000 psig. 1. Without stirring, k = 0.012 $min^{-1}$. 2.With stirring, k = 0.043 $min^{-1}$.

When no additional stirring was applied, there still was some mixing of the "reaction mixture" caused by the convection induced by the evolving molecular hydrogen. The impact of the forced stirring on the dissolution rate was apparent in the experiments. Forced stirring accelerates dissolution of uncoated aluminum powders by a factor of ca. 1.5. For coated powders which float on the surface of NaOH solutions, the increase in the dissolution rate under forced stirring reaches a factor of about 3.

## 2.4 Morphology of the Polymeric Films by Environmental Scanning Microscopy

Environmental Scanning Electron Microscope (ESEM) coupled with the Energy Dispersive X-ray (EDX) detector is a powerful tool for the characterization and examination of thin films. This technique was employed to study the coated particle shapes and structures as well as the elemental composition and the distribution of the elements within a coated particle.

ESEM is one of the best techniques to reveal the surface topography of solid particles. ESEM can detect the micro structure and produce micrographs. An ElectroScan 2020 model ESEM was employed in this study. Non-conductive samples measured with ESEM undergo charging which results in the image distortion and thermal damage.

To increase the electrical and thermal conductivity and, therefore, to reduce the electric charge caused by the high energy electron beam, a stub with gold coating on the surface was used. A double-sided adhesive tape was placed on the surface of the stub, then small amount of the sample was sprinkled on the double-sided tape and the loose portion of the sample was removed by a clean gas. Then the stub with the sample was placed in the operating chamber. The chamber was brought to atmosphere before opening the door. The position of the sample was adjusted in the x, y and z direction, as well as by rotation and tilting (Thornton, 1968).

Electron beam generated by the electron gun traveled towards and passed though the demagnifying lenses, beam-defining apertures and scanning coils. A fine beam was produced with diameter of about 100 Å (Wells *et al.*, 1974). When the sample is hit by the finely focused electron beam, several different kinds of signals are generated, such as secondary electrons, primary backscattered electrons, characteristic X-rays and

other types of radiation. The low energy secondary electrons are collected to form the image. This image is the most generally used technique to study the surface topography. The secondary electron emission is the process in which low energy (less than 50 eV) electrons are emitted from a solid when hit by higher energy electrons. In the traditional SEM, high vacuum in the operating chamber is required. But ESEM allows the observation of the sample image at relative low vacuum (ca. 5 Torr).

The function of the ESEM is to obtain the overall image of the sample and EDX can give the quantitative measurement of the sample and also the important information about the chemical composition. When the primary beam interacts with the sample, electrons are emitted from the inner shells of the sample atoms, the resulting vacancies are then filled by higher energy electrons from other shells. These atoms must release some of their energy when their electrons drop to lower energy levels. The energy is released as electro-magnetic radiation photons. The energy of the emitted radiation is equal to the energy difference between the two energy levels.

Since this energy difference for inner shells is very large, the radiation appears as X-rays. X-ray energies are intimately related to the atomic structure of the substance that emits them and each element emits a different pattern of X-rays (Hayat, 1974). The emitted X-rays can be sorted according to their energy and analyzed. Table 2.4 lists the X-ray emission lines of the elements used in this study.

**Table 2.4** X-ray Emission Lines for Al and Br elements (in keV)

| Element | $K_\alpha 1$ | $K_\alpha 2$ | $K_\beta 1$ | $L_\alpha 1$ | $L_\alpha 1$ | $L_\beta 1$ |
|---|---|---|---|---|---|---|
| Al | 1.48670 | 1.48627 | 1.55745 | | | |
| Br | 11.9242 | 11.8776 | 13.2914 | 1.48043 | 1.48043 | 1.52590 |

## 2.5 Materials Used

Aluminum powder, particle diameter 20 μm (Aldrich); Sodium hydroxide, 20-40 mesh beads, 97% (Aldrich); Dichloromethane (methylene chloride), 99.9%, A.C.S. HPLC grade (Aldrich); Polystyrene (**PS**), ave. $M_w$ ~280,000 (Aldrich); Poly(4-bromostyrene) (**PBS**), ave. $M_w$ ~65,000 (Aldrich); Poly(4-vinylbiphenyl) (**PVB**), ave. $M_w$ ~115,000 (Aldrich); Poly(styrene-*co*-methyl methacrylate) (**PSMMA**), $M_w$ ~100,000-150,000, ~40% styrene (Aldrich); Poly(4-vinylpyridine) (**PVP**), ave. $M_w$ ~160,000 (Aldrich); Poly(ethylene terephthalate) (**PETP**) (Aldrich); Poly(vinyl chloride-*co*-vinyl acetate) (**PVCVA**), ave. $M_n$ ~27,000, vinyl chloride content 86 wt. % (Aldrich); Poly(methyl methacrylate) (**PMMA**), ave. $M_w$ ~120,000, contains <5% of toluene (Aldrich); Poly(vinylidene fluoride-*co*-hexafluoropropylene) (**PVFH**), ave. $M_w$ ~400,000, ave. $M_n$ ~130,000 (Aldrich); Poly(vinylidene fluoride) (**PVF**), ave. $M_w$ ~180,000 (Aldrich); Polyisobutylene (**PIB**), ave. $M_w$ ~420,000 (Aldrich). Supercritical grade carbon dioxide (Matheson Co.) was purchased in cylinders pressurized by helium to 800-1400 psig.

# CHAPTER 3

# RESULTS AND DISCUSSION

## 3.1 Protective Properties of Polymeric Films Coated from SC $CO_2$

To demonstrate protective properties of polymeric films deposited from SC $CO_2$ and to compare the protection provided by different polymers, samples coated by eleven polymers under the chosen standard conditions (reactor temperature 170 °C, deposition pressure 4000 psig and the discharge temperature 60 °C), were prepared. The protective properties of these films were evaluated. The dissolution rate constants obtained by the fitting of the experimental dissolution kinetic curves was used as a quantitative measure of the protective properties of the polymeric films.

In the experiments, it was observed that the uncoated Al powder particles in alkali solutions all sink to the bottom and produce hydrogen very quickly (in 1.5 minutes). The dissolution curves were fitted by the function given in equation 4 and the dissolution constants of 0.080 $min^{-1}$ and 0.053 $min^{-1}$ were obtained for uncoated samples with and without forced stirring, respectively. For coated particles, it was apparent that a fraction of the sample is floating on the surface of the solution and releases hydrogen more slowly.

Figures 3.11-3.13 show the dissolution curves for some of the samples coated with PSMMA, PVP and PBS. The dissolution rate constants range from 0.014 $min^{-1}$ to 0.043 $min^{-1}$ under the well-stirred conditions. The samples with coating have much smaller dissolution rate constants than the uncoated one. It is obvious that the polymeric coating provide protection of the Al powder.

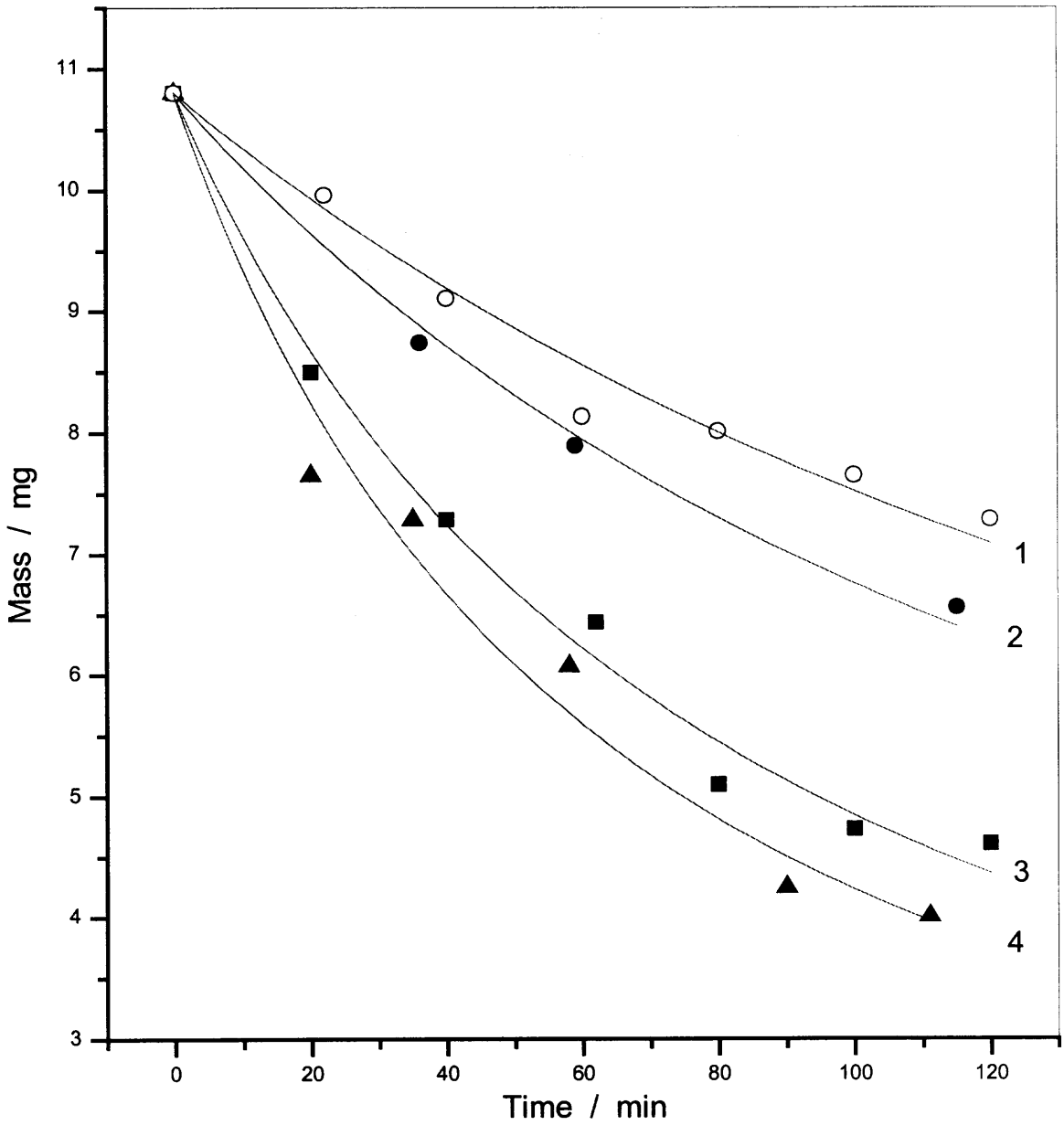


**Figure 3.11** Dissolution kinetics of Al powder coated with PSMMA in 0.01M, 40 mL NaOH: 1. Coated samples produced from $CH_2Cl_2$, x = 0.001, without stirring, k = 0.0043 $min^{-1}$. 2. Samples coated from SC $CO_2$ at 170 °C,, without stirring, k = 0.0059 $min^{-1}$. 3. The same sample as 1, with stirring, k = 0.012 $min^{-1}$. 4. The same sample as 2, with stirring, k = 0.014 $min^{-1}$.

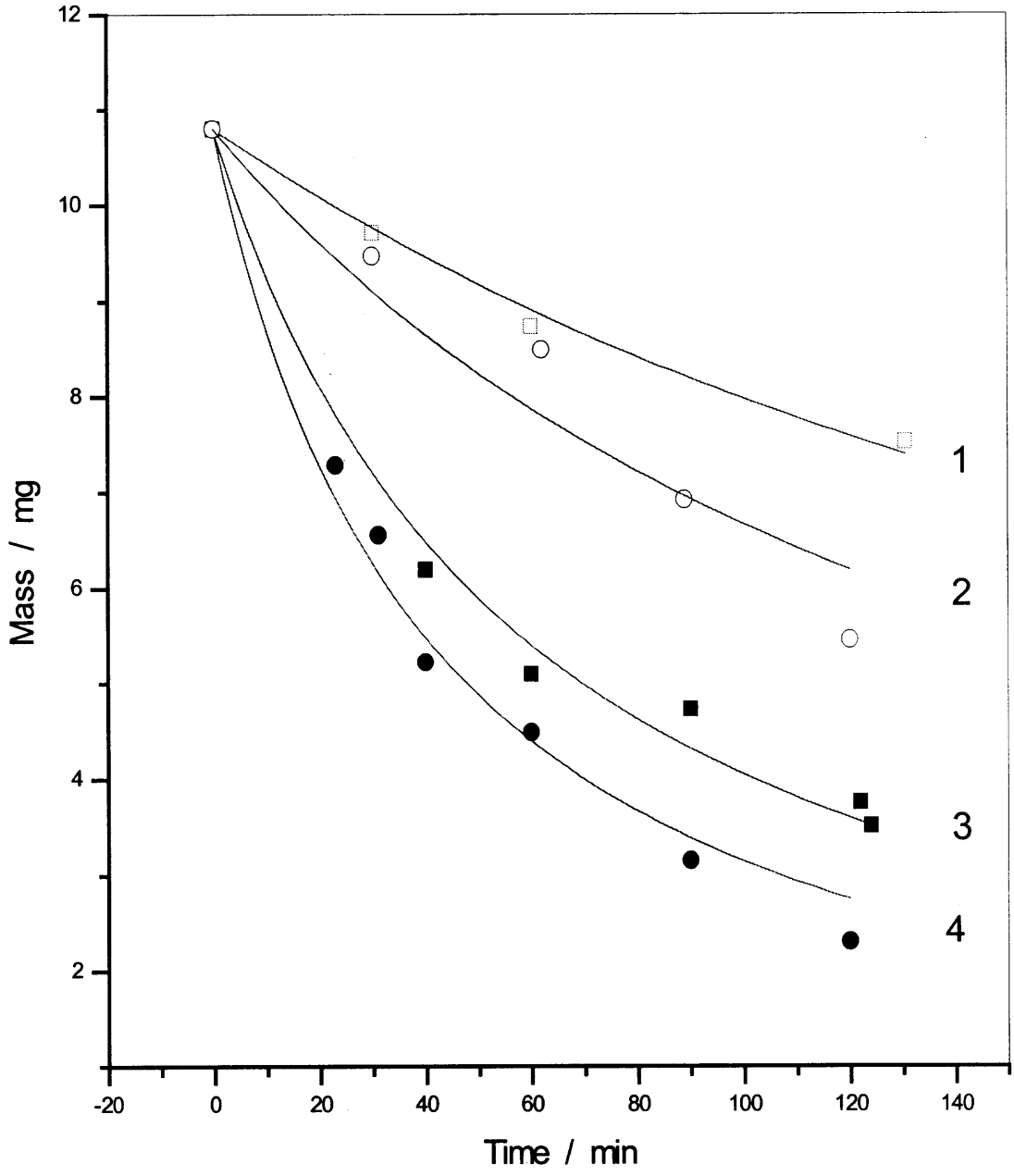


**Figure 3.12** Dissolution kinetics of Al powders coated with PVP in 0.01M, 40 mL NaOH: 1. Samples produced from $CH_2Cl_2$, x = 0.001, without stirring, k = 0.0035 $min^{-1}$. 2. Samples produced in SC $CO_2$ at 170 °C and 4000 psig, without stirring, k = 0.0067 $min^{-1}$. 3. The same sample as 2, with stirring, k = 0.017 $min^{-1}$. 4. The same sample as 1, with stirring, k = 0.024 $min^{-1}$.

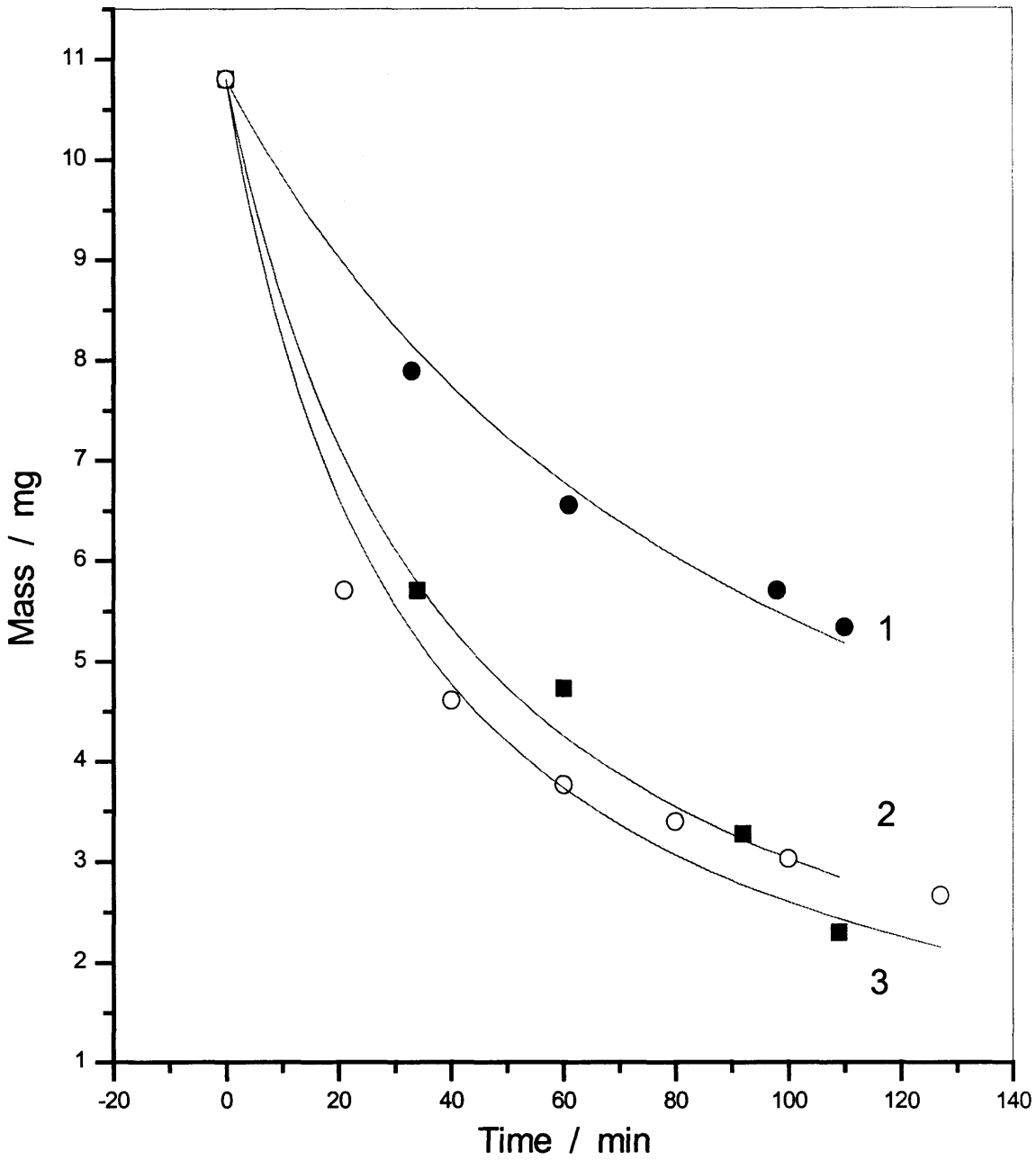


**Figure 3.13** Dissolution kinetics of Al powders coated with PBS in 0.01M, 40 mL NaOH: 1. Coated samples produced in $CH_2Cl_2$, x = 0.001, without stirring, k = 0.0066 $min^{-1}$. 2. Sample coated from SC $CO_2$ at 170 °C and 4000 psig, with stirring, k = 0.026$min^{-1}$. 3. The same sample as 1, k = 0.031 $min^{-1}$, stirring was used.

The samples coated with the other eight polymers also exhibit similar protective properties. For the polymers having strong absorption in the UV region, the thickness of the films were determined using UV spectroscopy. The results are collected in Table 3.1. In addition, this table contains data on the dissolution rate constant for powders with polymeric films deposited from organic solvents with controlled mole fractions of the monomer units of the polymers (x = 0.001). Analysis of the data from Table 4 shows that for the majority of the polymers deposited from SC $CO_2$ at the standard conditions, the typical polymeric film thickness is from 2 to 20 nm. The measured film thickness for PSMMA was 80 nm.

**Table 3.1** Dissolution Rate Constant for Samples (in NaOH: 0.01 M, 40 mL) Coated from Supercritical Carbon Dioxide and Organic Solvents

| Polymers | Sample Coated from SC $CO_2$ | | | Sample Coated from Organic Solvent, with A Mole Fraction 0.03 | | |
|---|---|---|---|---|---|---|
| | Average Film Thick-ness / nm | k / $min^{-1}$ | | Average Film Thick-ness / nm | k / $min^{-1}$ | |
| | | No stirring | With stirring | | No stirring | With stirring |
| PVP | 6.2 | 0.0062 | 0.017 | 37.0 | 0.0035 | 0.024 |
| PVB | 3.2 | 0.014 | 0.038 | 60.6 | 0.011 | 0.032 |
| PBS | 2.7 | 0.0098 | 0.026 | 61.4 | 0.0066 | 0.031 |
| PS | 22 | 0.014 | 0.042 | 33.4 | 0.0068 | 0.025 |
| PSMMA | 80 | 0.0060 | 0.014 | 20.5 | 0.0043 | 0.012 |
| PIB | 2.2 | 0.0043 | 0.024 | 8.5 | 0.0077 | 0.022 |
| PVF | | 0.014 | 0.032 | 20.3 | | |
| PVFH | | 0.0081 | 0.015 | 28.3 | | |

**Table 3.1** Dissolution Rate Constant for Samples (in NaOH: 0.01 M, 40 mL) Coated from Supercritical Carbon Dioxide and Organic Solvents (Continued)

| | | | | | | |
|---|---|---|---|---|---|---|
| PMMA | | 0.0055 | 0.017 | | 0.0064 | 0.0097 |
| PVCVA | | 0.0061 | 0.023 | 16.8 | 0.022 | 0.040 |
| PETP | | 0.0040 | 0.011 | 47 | | |
| PVA | | | | 24.3 | 0.018 | |
| Uncoated Al powder | | 0.053 | 0.080 | | | |

All the samples coated in SC $CO_2$ demonstrated decreased dissolution rate constant compared with the uncoated Al powder. The dissolution rate constants for the coated powders are 2 - 13 times lower than that of the uncoated Al powder. The films deposited from SC $CO_2$ also demonstrate improved protective properties comparable with the films deposited from organic solutions, despite the much thicker average film thickness of the latter ones. The possible reason for this is that the thick polymeric films deposited from organic solutions are not uniform. Among the polymers used in the current study, PVP has the best protective properties and also relatively strong UV absorption, which leads to a convenient and sensitive measurement of the film thickness. Due to these reasons, PVP was chosen as the coating material in the further detail studies.

### 3.2 Dependence of the Film Properties on the Deposition Temperature

As mentioned before, the experimental conditions can be changed by either altering temperature or pressure to adjust the density and the solvating power of supercritical carbon dioxide. The combination of the optimal temperature and pressure leads to the optimal deposition conditions. In this section, the effect of the reactor temperature on the

properties of the deposited films is discussed. To study the effect of the reactor temperature on the coating properties, poly (4–vinyl pyridine) was chosen as the coating material for the reason mentioned in section 3.1. Aluminum powder was coated with PVP at different temperatures from 80 to 210 °C. During the coating process, the final pressure and the discharge temperate were kept constant (p = 5800 psig and discharge temperature = 60 °C) to make the reactor temperature an exclusive variable in this series of trials. The film thickness and the dissolution rate constants were obtained using the method described earlier. Figures 3.21 and 3.33 show the relationship between the dissolution rate constant and the deposition temperature.

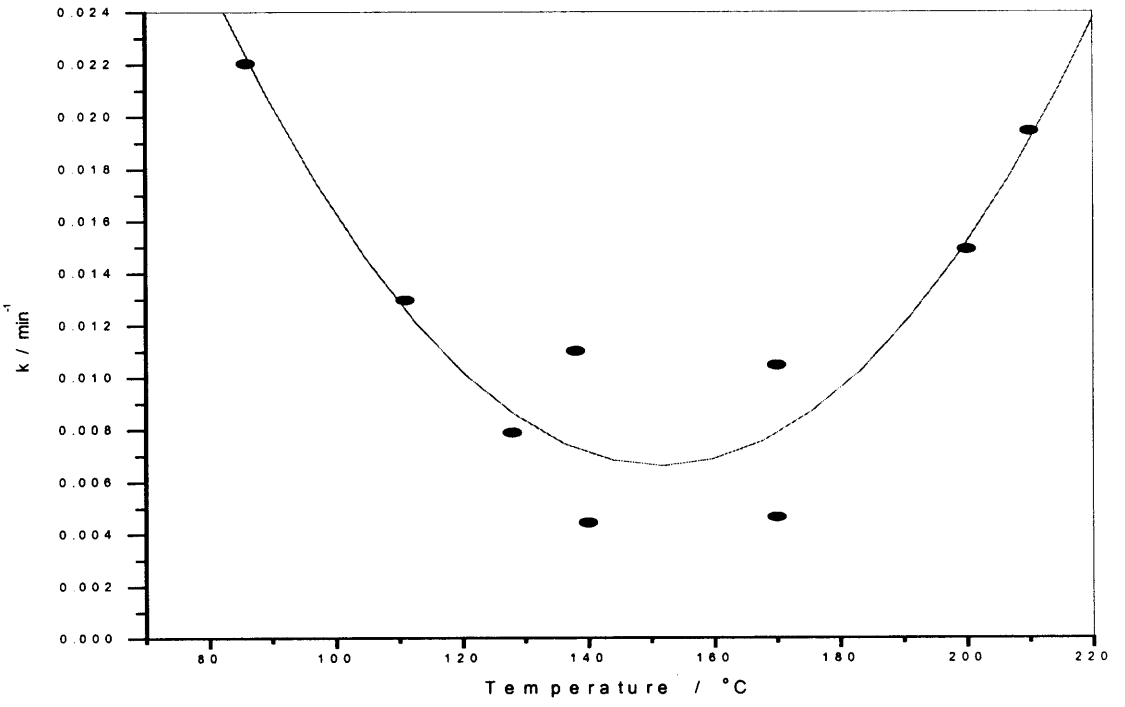


**Figure 3.21** Temperature dependence of the dissolution rate constant for coated Al powders coated with PVP at 5500 - 5800 psig in SC $CO_2$. No stirring was used in the dissolution measurements.

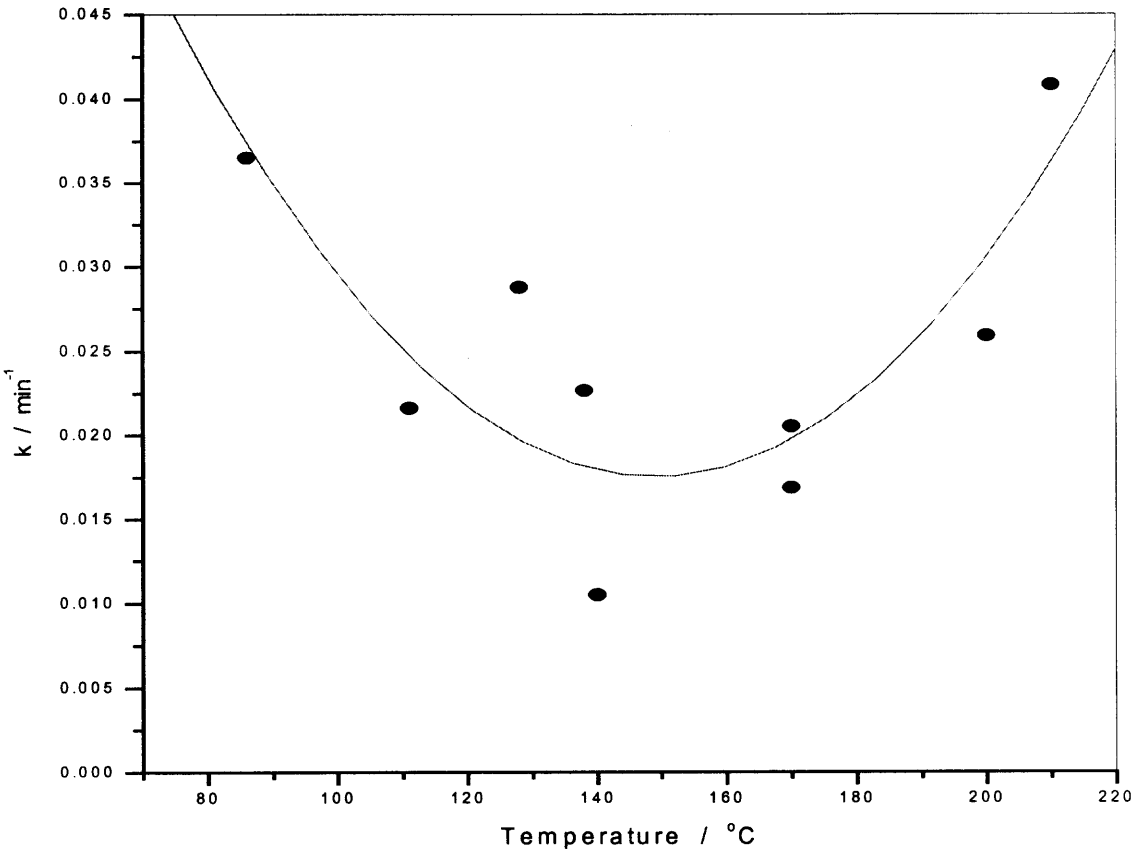


**Figure 3.22** Temperature dependence of the dissolution rate constant for coated Al powders coated with PVP at 5500 - 5800 psig in SC $CO_2$. Stirring was used in the dissolution measurements.

It was found that the dissolution rate constants first decreases with temperature, but when the temperature reaches a certain point, the dissolution rate constant starts to increase with temperature. The isobaric increase of the reactor temperature in the range 80 – 140 °C was found to result in the decrease of the dissolution rate constant, meaning the improvement of the protective properties with the deposition temperature. This effect is similar to that obtained for aluminum powders coated with poly (4-vinyl biphenyl) (PVB). It was explained by the increase of the polymer's solubility in supercritical carbon dioxide with temperature at a constant pressure. Further increase of temperature leads to the thermal destruction of the polymer.

This turning point temperature is around 140 ° C. When the temperature is above this point, the polymer destruction begins. When temperature is increased to ca. 180 °C, the residual polymer in the reactor turned to brown color. This indicates thermal destruction of the polymer, which explains the increased dissolution rate constant when the deposition temperature was above 150 °C.

It should be noted that the dissolution rate constant did not decrease with the increase of the film thickness. There are two possible explanations of the observed change in the protective properties with the deposition temperature, depending on the mechanism of the polymer transfer. The first one is the solubility mechanism. It is based on the assumption that the films are produced from the polymer which was dissolved in SC $CO_2$.

There are two main factors affecting solubility, the vapor pressure of the solute (polymer) and the density of the solvent (SC $CO_2$). The increase of temperature at a constant pressure leads to an increase of the solute vapor pressure and to a decrease in the solvent density. If the density effect predominates (which occurs at pressures close to the critical pressure), the solubility decreases with temperature. If the vapor pressure effect predominates (which occurs at pressures far above the critical pressure), the solubility increases with temperature. The relationships between the solubility and temperature for low molecular weight compounds are available in the literature. When pressure is above 150 atm, the solubilities of compounds increase with the increase of temperature (Yamini and Bahramifa, 2000; Kramer and Todos, 1989; Bratle *et al.*, 1991). For polymers, the relationship between the solubility and temperature is different. Since $CO_2$ is a very weak solvent for polymers, they in general have very limited solubility in SC $CO_2$ below 80 °C.

However, when temperature is above 80 °C, polymers have significant increase in the solubility at elevated temperatures and pressures in SC $CO_2$. The effect of temperature on the solubility of solids in SCF can be both negative and positive (McHuge and Paulaitis, 1980; Zhao *et al.*, 1995). In the previous studies in this laboratory, negative effect of temperature on the solubility of PVDF in SC $CO_2$ at pressure 200 atm was observed. However, for PVB, the effect of temperature on the solubility at pressure 345 atm is positive.

The second mechanism of polymer transfer is via aerosol-like particles. If polymer transfer occurs by this mechanism, large scattering of the experiment data on the film thickness could be anticipated. When this mechanism preveals, a polymer is not really dissolved in supercritical carbon dioxide but rather exists as an "aerosol". When supercritical carbon dioxide transports this "aerosol" into the sample volume, the polymer is deposited unevenly on the metal's surface and the film produced on the surface is not uniform.

It could be that both of the two mechanisms contribute to the polymer transfer. Aerosol-like particles could be large, which leads to an increase in the measured average film thickness but with a limited contribution to the protective properties. Truly dissolved polymer could form a thin uniform polymeric film around the metal particles, which gives lesser effect on the average film thickness, but larger contribution to the protective properties. Since the deposition temperature of 140 °C provided the lowest dissolution constant for Al powder coated with PVP, this temperature was chosen as the optimal temperature in the further detailed studies. Figures 3.23 and 3.24 show the dependence of dissolution rate constant on film thickness at different pressure.

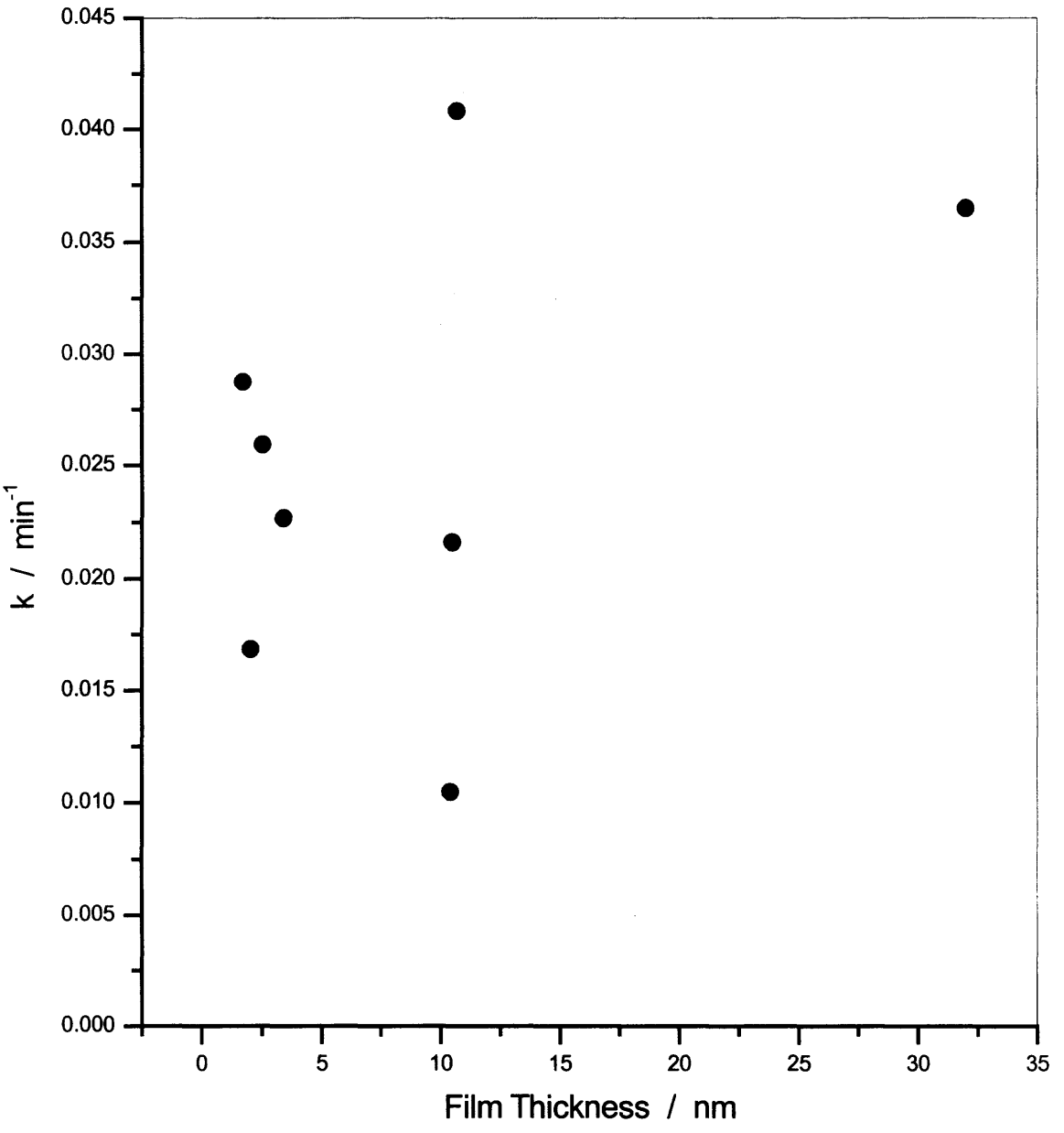


**Figure 3.23** Dissolution rate constant dependence of the PVP coated Al powders (10.8 mg) in NaOH (0.01 M, 40 mL) on the film thickness. Films deposited from SC $CO_2$ at different temperatures. Pressure 5400 psig. Stirring was used in the dissolution measurements.

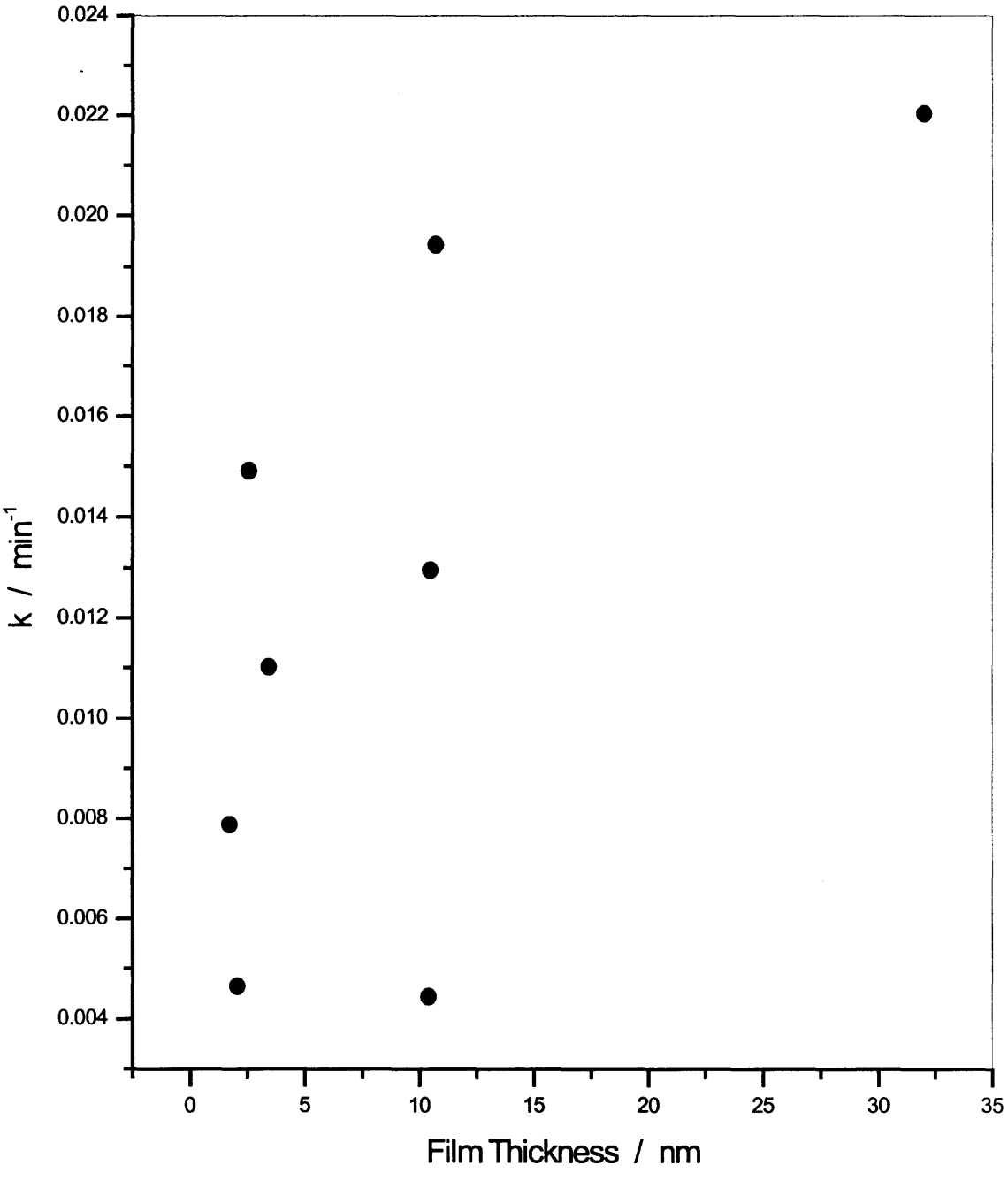


**Figure 3.24** Dissolution rate constant dependence of the PVP coated Al powder (10.8 mg) in NaOH (0.01 M, 40 mL) on film thickness. Films deposited from SC $CO_2$ at different temperatures. Pressure 5400 psig. No stirring was used in the dissolution measurements.

### 3.3 Dependence of the Film Properties on the Deposition Pressure

Since the pressure also has great impact on the polymer deposition, the pressure dependence on the dissolution rate constant was investigated. To make pressure the exclusive variable, the deposition temperature and the discharge temperature were kept constant. Since the previous study has already established the optimal deposition temperature for PVP deposition of 140 °C, this temperature was used as the deposition temperature (T = 140 °C and $T_{discharge}$ = 60 °C). The deposition pressures range in this study was from 80 atm to 480 atm. The results are shown in Figure 3.31 and 3.32.

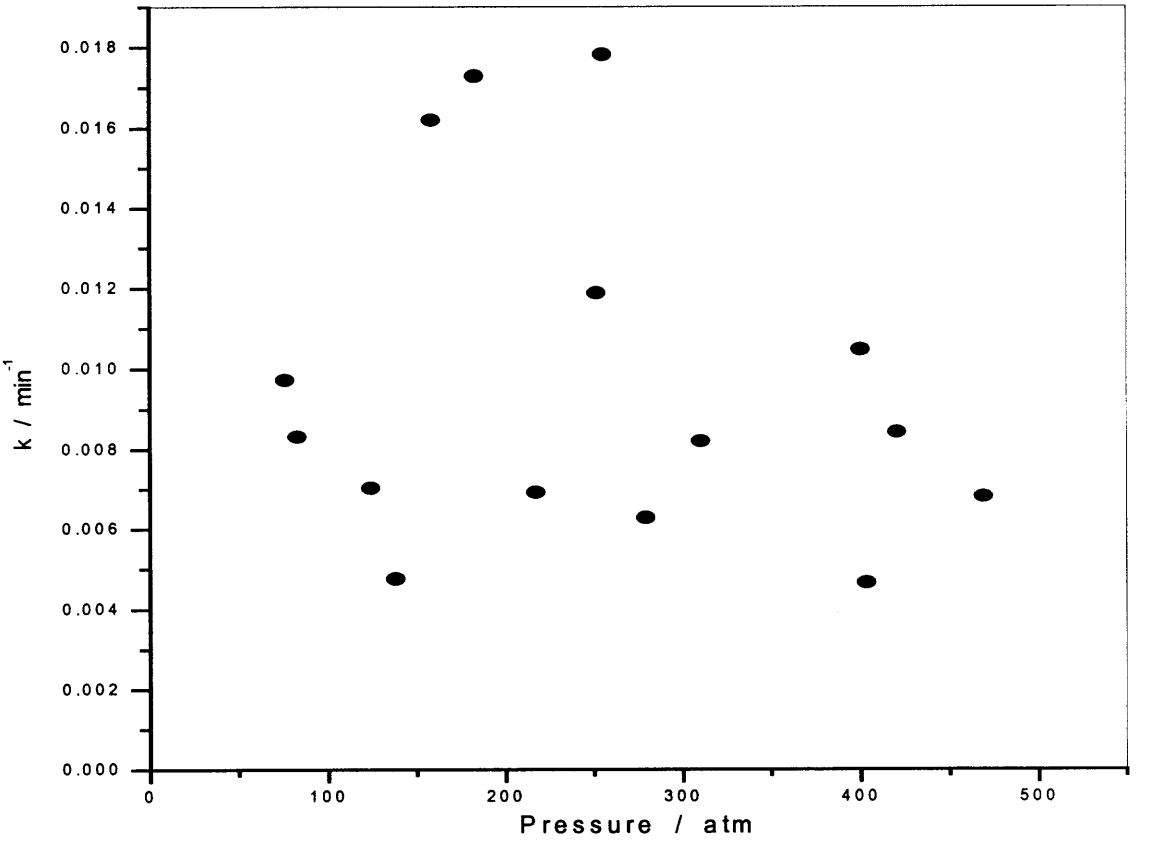


**Figure 3.31** Dissolution rate constant of PVP coated (SC $CO_2$, 170 °C) Al powder (10.8 mg) in NaOH (40 mL 0.01 M) vs. the deposition pressure. No stirring was used in the dissolution measurements.

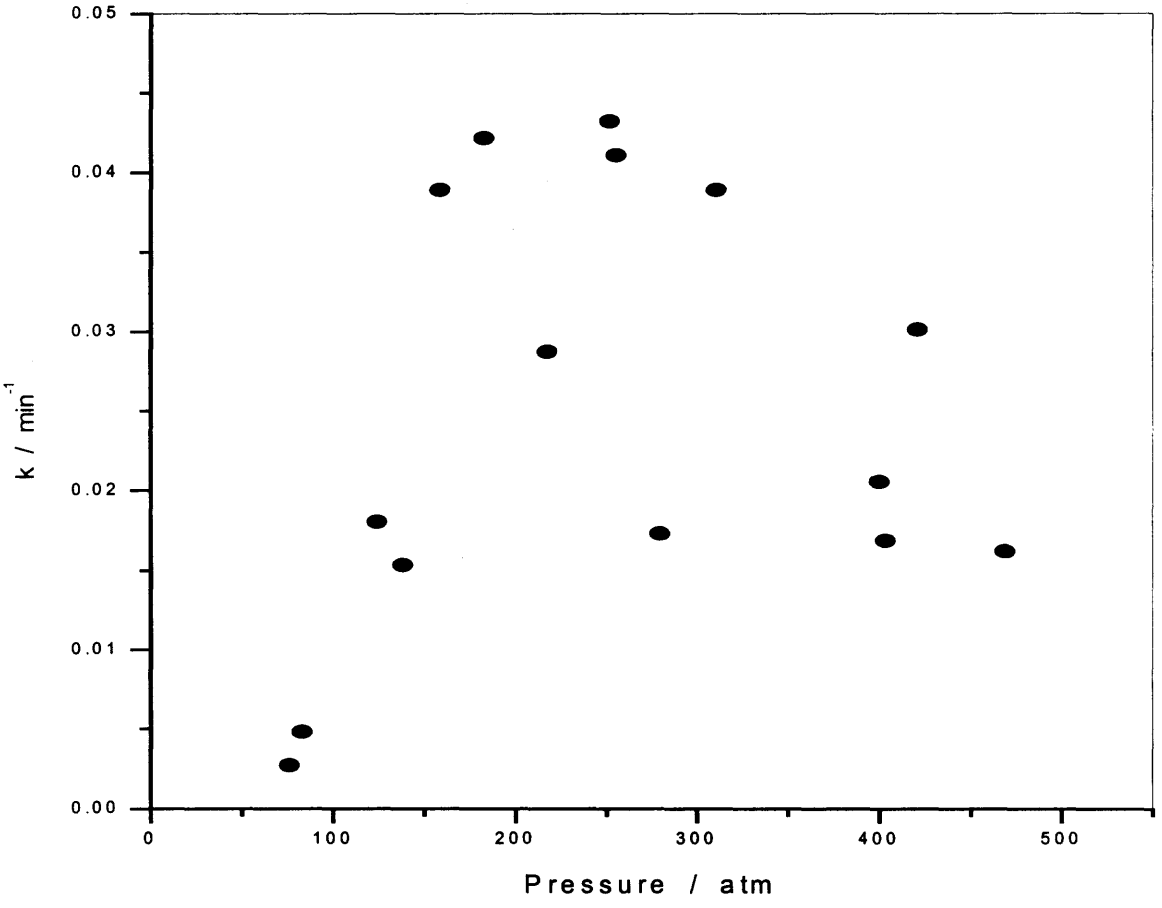


**Figure 3.32** Dissolution rate constant of the PVP coated (SC $CO_2$, 170 °C) Al powder (10.8 mg) in NaOH (40 mL 0.01 M) vs. the deposition pressure. Stirring was used in the dissolution measurements.

No certain conclusion on the pressure dependence could be derived due to the large scatter of the experimental points. The deposition pressure of 400 atm gives average dissolution rate constant k = 0.024 $min^{-1}$ and 0.0076 $min^{-1}$ for with and without forced stirring measurements, respectively. For p = 500 atm, the average dissolution rate constants are 0.016 $min^{-1}$ and 0.0070 $min^{-1}$ for "stirred" and "non-stirred" measurements, respectively. These rate constants are ca. 3 times lower than that for an uncoated powder.

The correlation between the dissolution rate constant and the film thickness is shown in Figures 3.33 and 3.34. Again, the scatter is significant. Figure 3.33 indicates improvement in the protective properties with the film thickness, as expected.

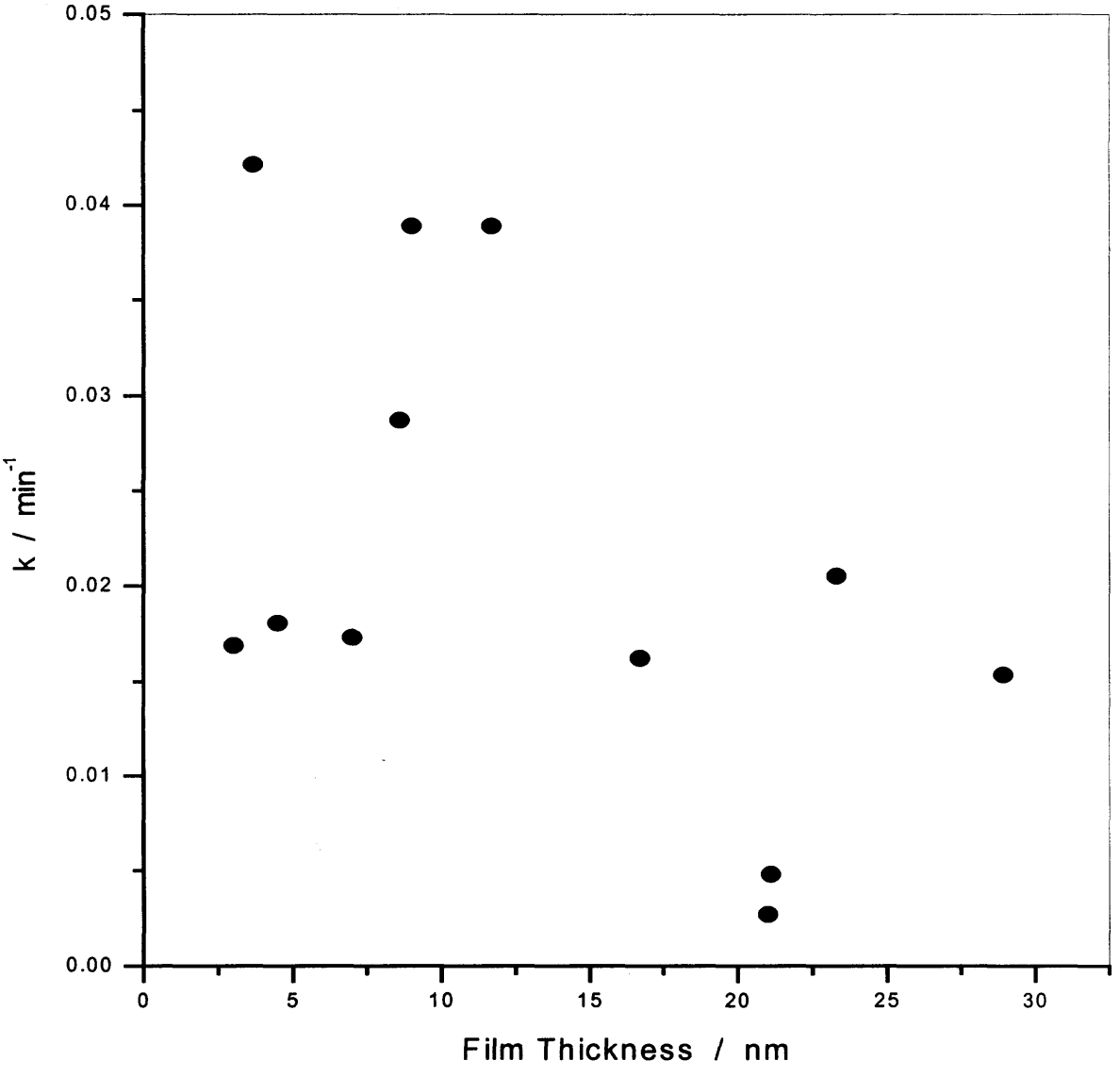


**Figure 3.33** Dissolution rate constant dependence of the PVP coated Al powder (10.8 mg) in NaOH (0.01 M, 40 mL) on film thickness. Films deposited from SC $CO_2$. Temperature 170 °C. Stirring was used in the dissolution measurements.

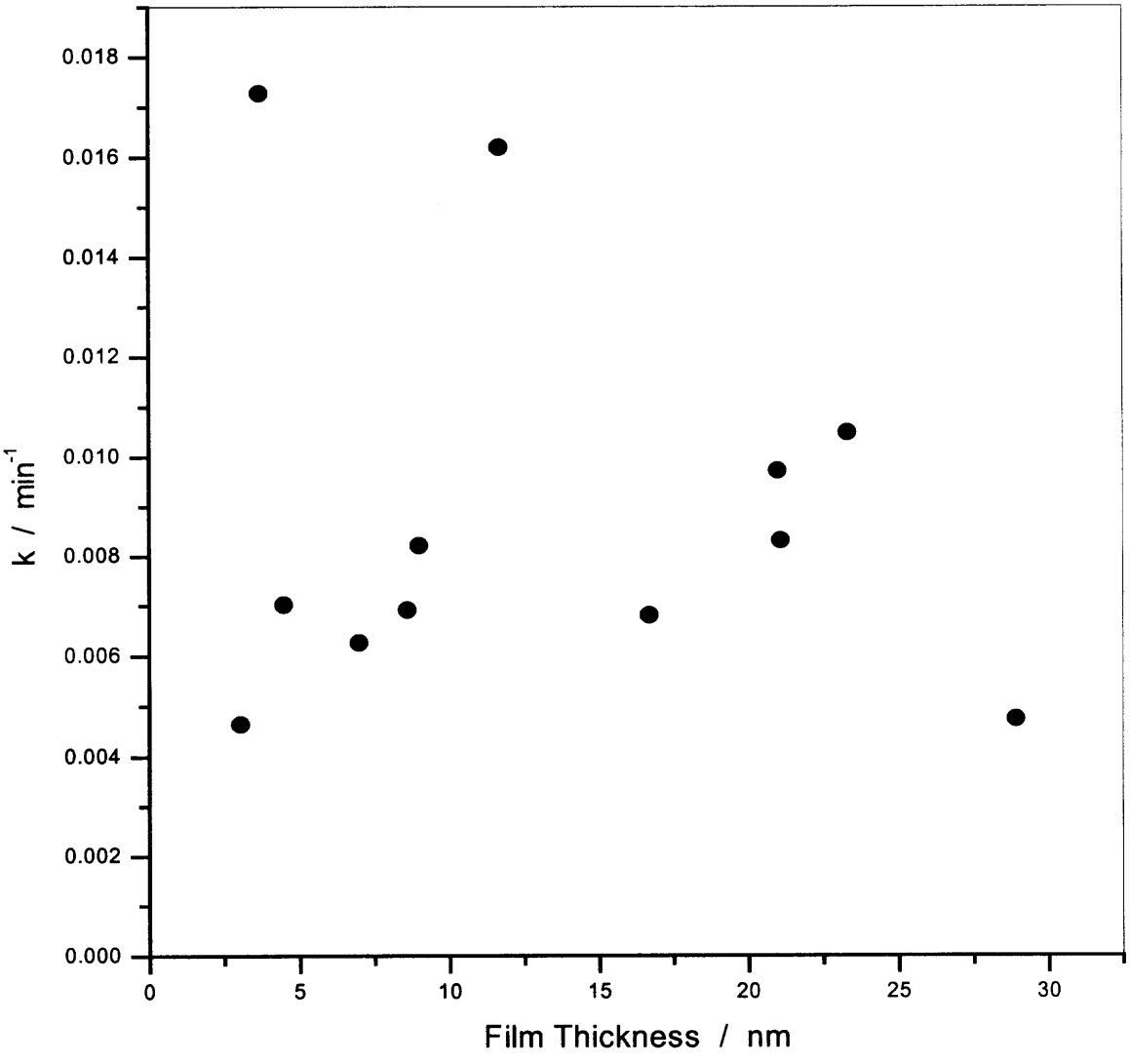


**Figure 3.34** Dissolution rate constant dependence of the PVP coated Al powder (10.8 mg) in NaOH (0.01 M, 40 mL) on film thickness. Films deposited from SC $CO_2$. Temperature 170 ° C. No stirring was used in the dissolution measurements.

The observed significant scatter of the experiment data could come from two aspects. First, the morphology of the polymer films could be different under different condition. Second, the polymeric films could be not uniform due to the low discharge pressure. When the deposition pressure was 150 atm, the discharge pressure was 85 atm.

If the deposition pressure was lower than 150 atm, the discharge pressure could be lower than the critical pressure of $CO_2$. Since the solving power of SC $CO_2$ has dramatic change at the near-critical region, when pressure is lower than critical pressure, the polymer precipitated in large amount before the discharge and produced rough "films" with irreproducible protective properties. Higher deposition pressures lead to the polymer precipitation only during the discharge, thus producing smoother films. Hence, to achieve better protective propertis, it is better to use higher pressures (above 400 atm). In the further studies, pressure of 500 atm was used.

### 3.4 Dependence of the Film Properties on the Discharge Temperature

The discharge temperature also was found to affect the coated sample's morphology, the protective properties and the film thickness. To investigate the dependence of the film properties on the discharge temperature, a series of experiments was carried out with the discharge temperature ranging from 40 °C to 120 °C and keeping the reactor temperature and pressure constant. The results are shown in figures 3.41 and 3.42. The dissolution rate constant decreases with increasing the discharge temperature from 40 °C to 60 °C and begin to increase after 60 °C. The film thickness, similarly to the cases discussed before, exhibits no dependence on the discharge temperature within the scatter of the data.

The reason for this result is simple. If SC $CO_2$ is discharged at a high temperature, most of the polymer is not deposited due to the almost equivalent solvent power of SC $CO_2$. In this discharge temperature range, the produced film thickness is small. When the discharge temperature is low enough, the solvating power of SC $CO_2$ decreases

significantly, and the most of the polymers is deposited on the surface of Al powder before the discharge, resulting in a large scatter of the average film thickness with irreproducible protective properties. Since the discharge temperature of 60 °C provided the best protective properties, this temperature was used as the optimal discharge temperature for the polymer coating.

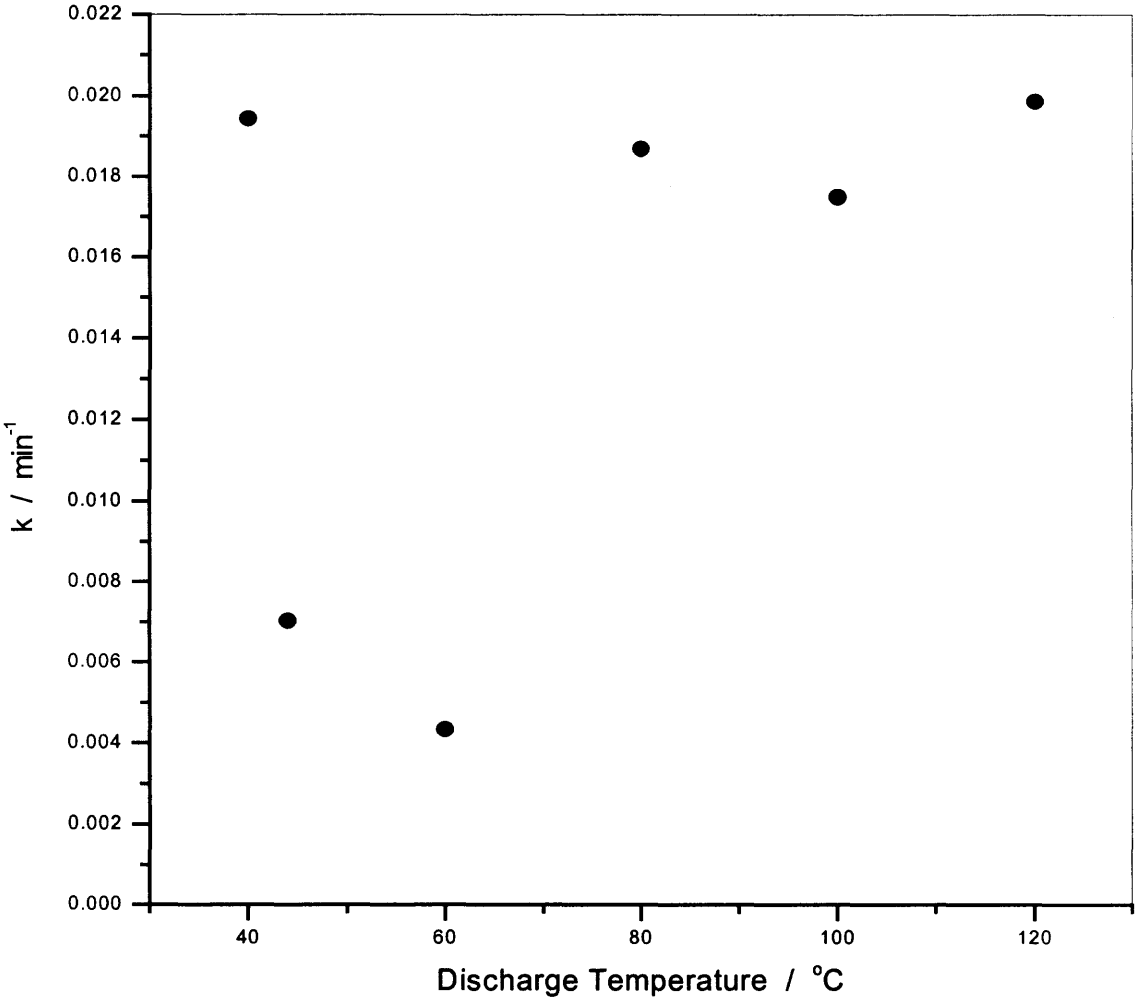


**Figure 3.41** Impact of the discharge temperature on the protective properties of the PVP coated Al powders coated in SC $CO_2$ at 5800 psig and 140 °C. No stirring was used in the dissolution measurements.

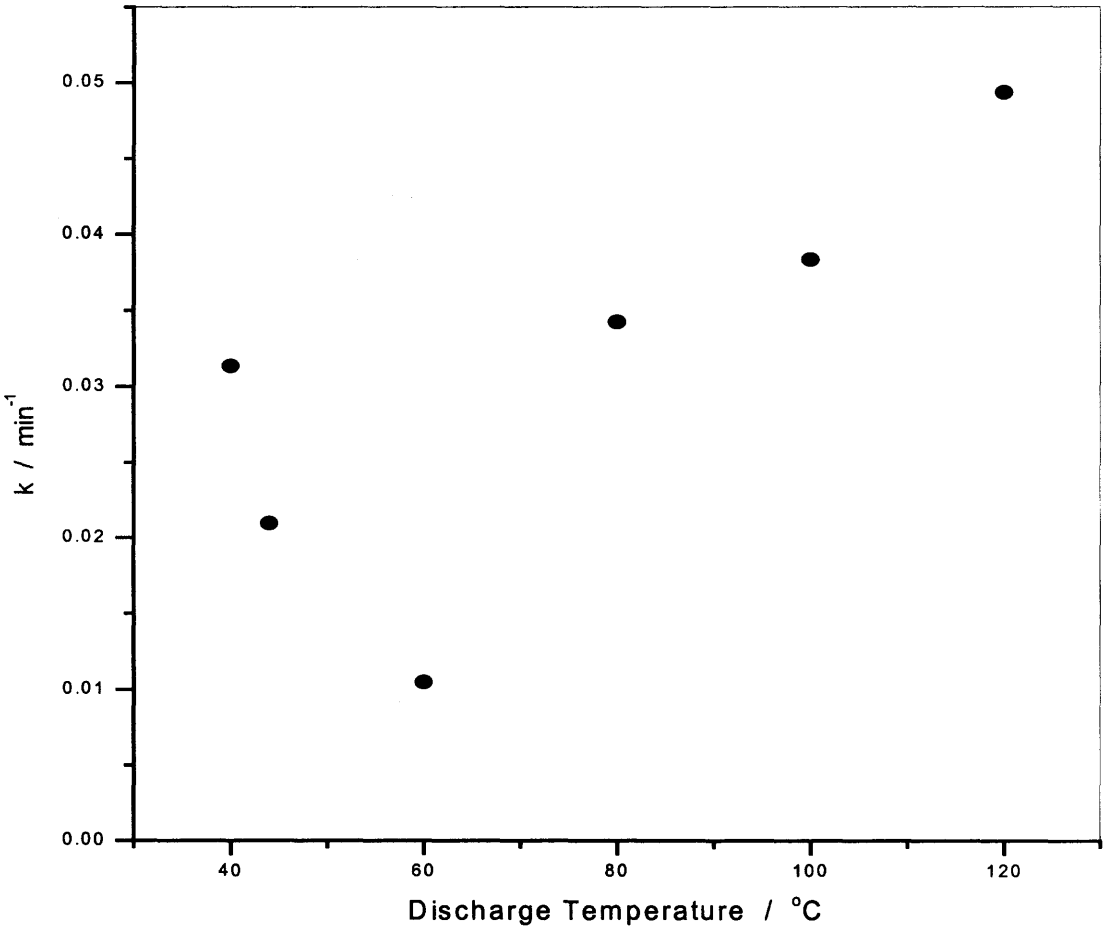


**Figure 3.42** Impact of the discharge temperature on the protective properties of the PVP coated Al powders coated in SC $CO_2$ at 5800 psig and 140 °C. Stirring was used in the dissolution measurements.

### 3.5 The Protective Properties of Polymers Coated from Organic Solutions

To study and compare the protective properties of polymer in alkali, all the polymers under the study were coated on the surface of aluminum powder from an organic solvent to form a film with a certain targeted thickness. In this study, the targeted film thickness of 20 nm was chosen as a "standard thickness". To produce the expected film thickness, polymers were dissolved in an appropriate solvent to make a 0.001 M concentration. Then by using Equation 2, the volume of the needed polymer solutions was calculated.

Aluminum powder was immersed in the polymer solutions of a known volume, after which the organic solvent was evaporated, and a ca. 20 nm films were formed on the surface of the Al powder.

To verify the film thickness, all coated Al powders were checked by repeating the steps described in chapter 2.2. The results were satisfactory. All the film thickness were equal or very close to 20 nm within ± 2 nm. The samples were characterized using the dissolution rate constant. The dissolution was performed in two ways: with stirring by a magnetic bar and without stirring. Since the measurements with stirring provide better reproducibility, the results obtained with stirring were used.

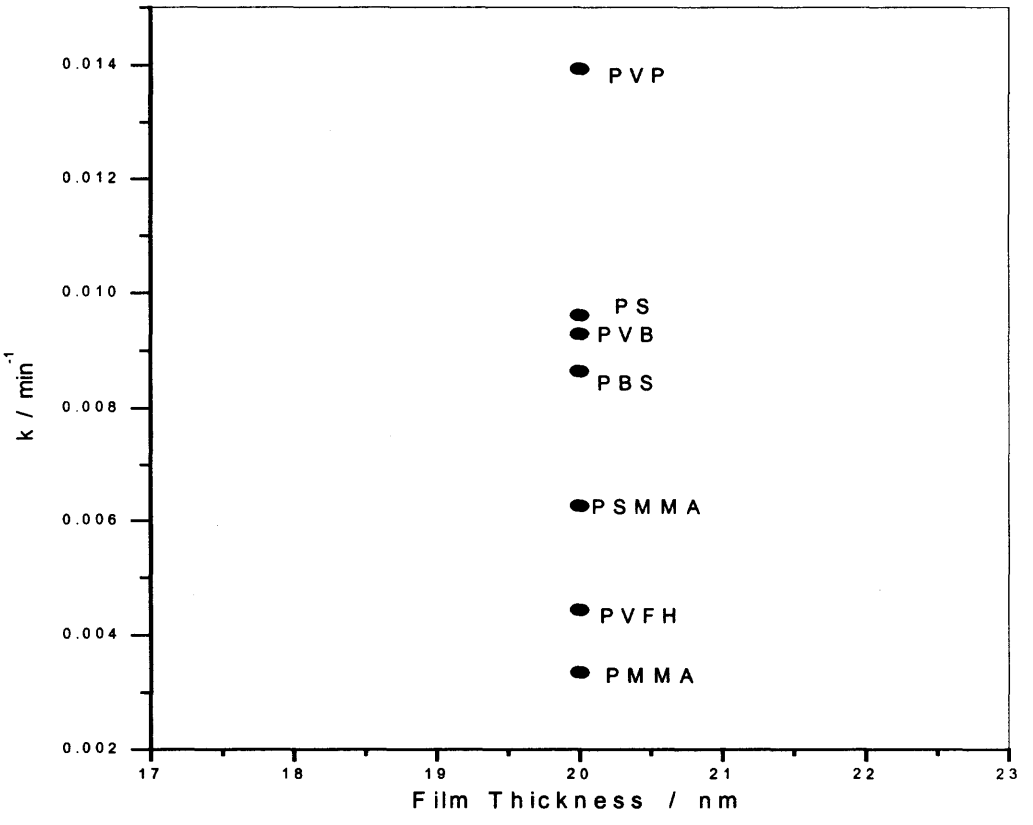


**Figure 3.51** Dissolution rate constants in NaOH (0.01 M, 40 mL) for samples (10.8 mg) coated with different polymers in organic solvents. Average polymer film thickness were ca. 20 nm for all samples. No stirring was used in the dissolution.

The polymers' resistance to alkali is illustrated in Figure 24. Among the polymers, PSMMA, PMMA and PVFH have better protective properties. This can be explained by the fact that PSMMA and PMMA and PVFH have the lowest critical surface tension. Critical surface tension is a measure of the degree of the wettability of the polymer surface. Several plausible correlations between the protective properties of the films and the physical properties of the polymers were suggested and verified. Figure 3.52 shows the correlation of k with the critical surface tension of the polymers.

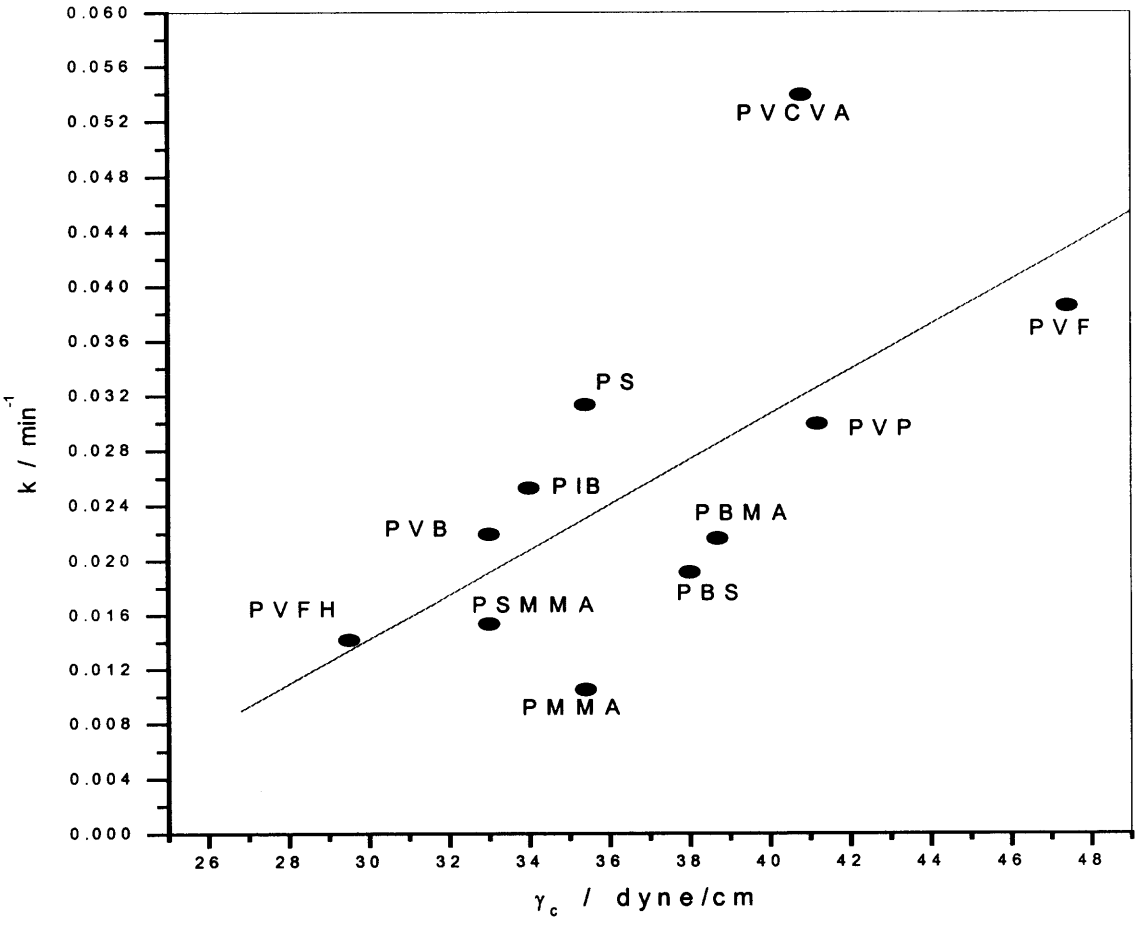


**Figure 3.52** Correlation of the critical surface tension of the polymers and the dissolution rate constant of coated samples.

Polymers with lower critical surface tension (with less wetting ability) demonstrate better protective properties. The critical surface tension is being considered as a criterion for the polymer selection. This criterion will be further verified in the future experiments.

To study the relationship between the protective properties and the film thickness, a set of samples which satisfy a set of specific requirements was prepared. The requirements include smooth surface and a large range of the thickness of the films. Since coating in SC $CO_2$ produces polymeric film with large scatter and can not produce thick films, the samples were prepared by immersing Al powder in polymer's organic solution and subsequent evaporating organic solvent. Samples with the targeted film thickness of 1, 2, 3, 5, 8, 10, 20, 40, 60 and 100 nm of PVP films were prepared.

Figures 3.53 and 3.54 show the relationship between the dissolution rate constant and the film thickness. Increasing the film thickness significantly influences the dissolution rate constant when the film thickness is less than 20 nm. From 1 nm to 20 nm, the dissolution rate constant decreases sharply with the film thickness. When the film thickness is larger than 20 nm, the decrease of the dissolution rate constant with film thickness slows down. When the film thickness reaches 100 nm, the dissolution rate constant of coated Al powder depends weakly on the film thickness.

Based on Figures 3.53 and 3.54, when the film thickness is above 20 nm, the increase of the film thickness leads to a small change of the protective properties. It is evident that for a good protection, 20 nm film thickness is a suitable choice. Further increase of film thickness is not necessary.

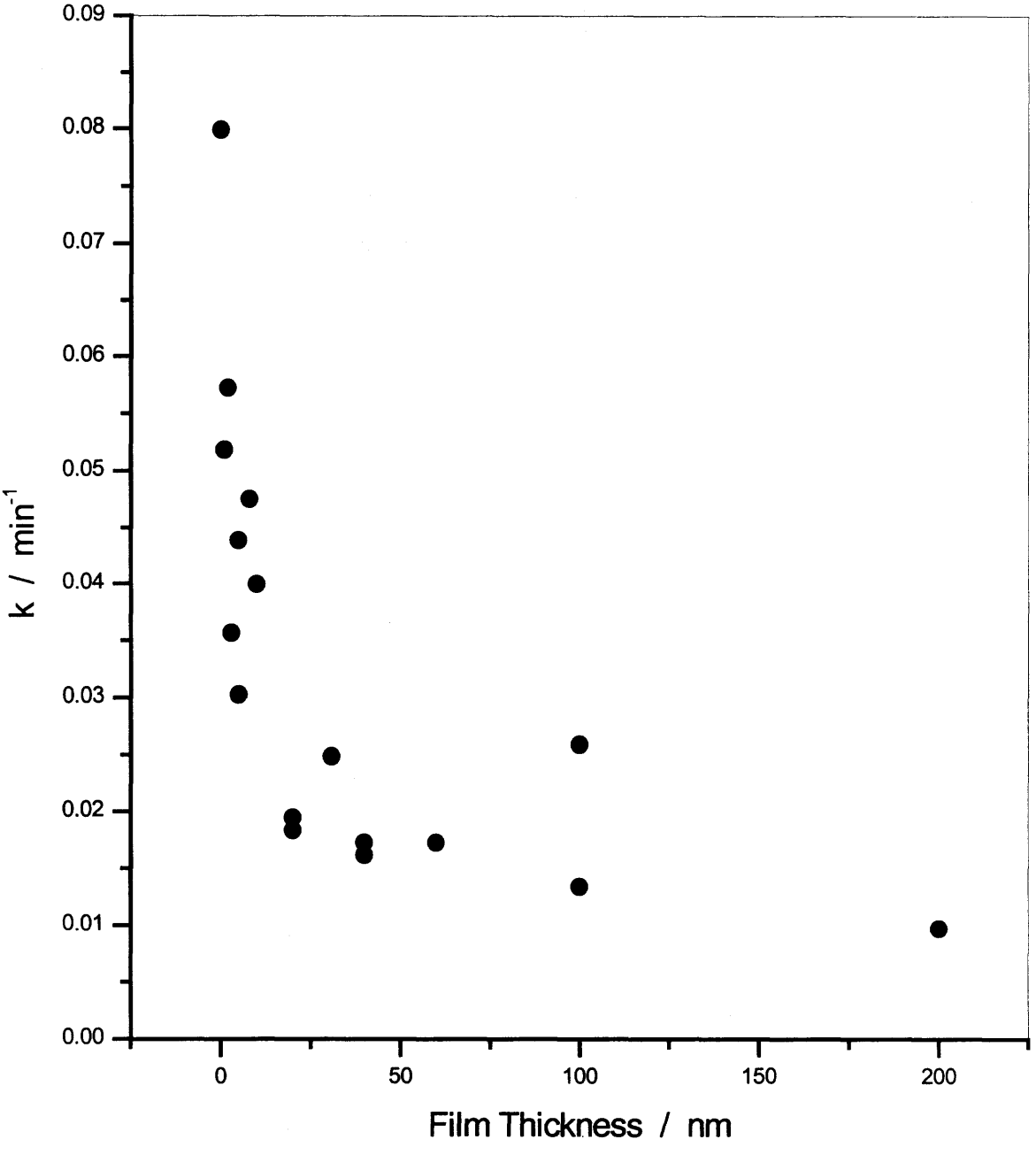


**Figure 3.53** Rate of dissolution (10.8 mg Al powders in 40 mL 0.01 M NaOH) vs. film thickness. Stirring was used in the dissolution measurements. Aluminum powders was coated with PVP (from $CH_2Cl_2$). Film thickness estimation using UV spectroscopy.

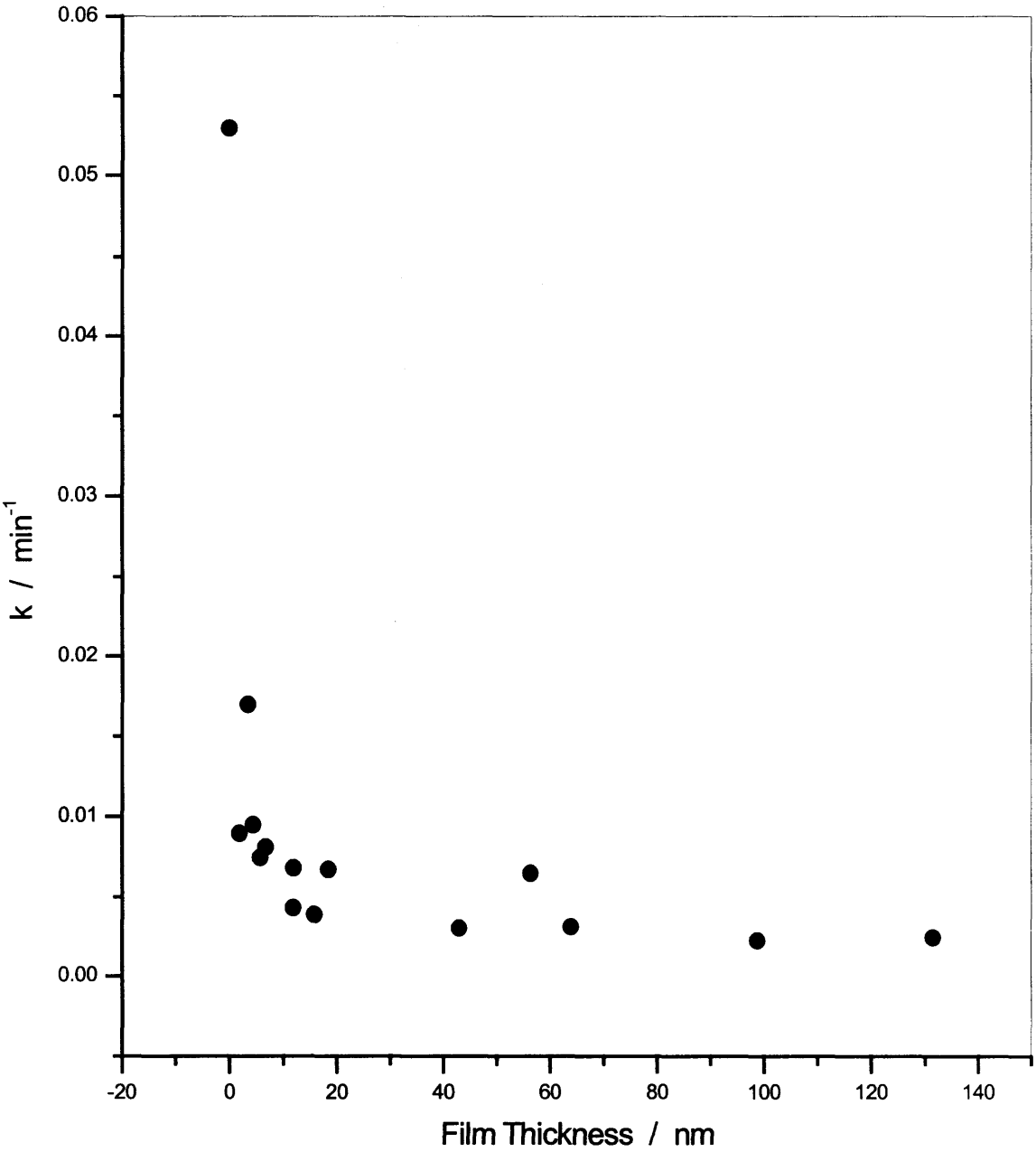


**Figure 3.54** Rate of dissolution (10.8 mg Al powders in 40 mL 0.01 M NaOH) vs. film thickness. No stirring was used in the dissolution measurements. Aluminum powders was coated with PVP (from $CH_2Cl_2$). Film thickness estimation using UV spectroscopy.

Since the increase of the film thickness leads to the decrease of the dissolution rate constant, it is reasonable to expect that with a thick enough polymer film, a coated sample can be completely protected. In order to verify this assumption, samples with film thickness of 0.5 $\mu$m were prepared and the dissolution in NaOH (0.01 M, 40 mL) was investigated. The masses of the residual aluminum powders were measured at the 30, 60, 90 and 120 minutes time intervals and were corrected for the mass loss due to washing. After the mass loss correction, it was found that all the data are close to the original mass, either with-stirring or without stirring dissolution.

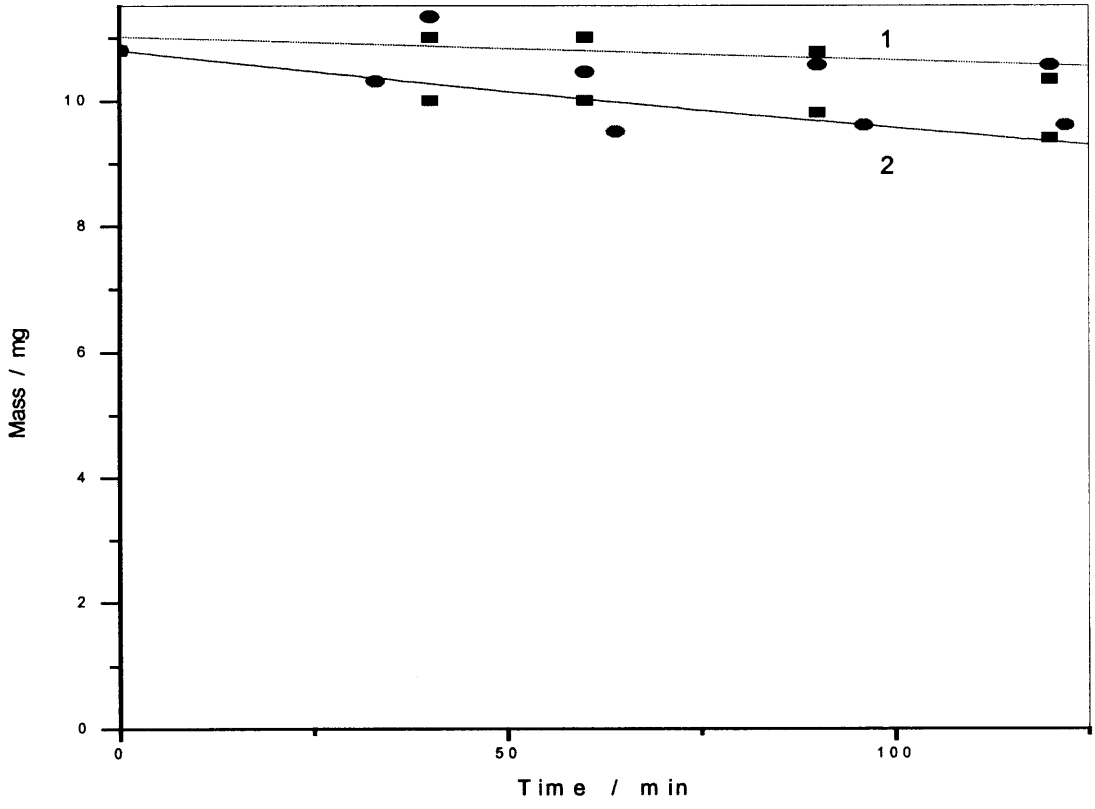


**Figure 3.55** Dissolution kinetics of Al powders (10.8 mg) coated with PMMA (ave. film thickness 0.5 um) from $CH_2Cl_2$ in NaOH (40 mL, 0.01 M). 1 - after the mass loss correction; 2 – before the mass loss correction. Oval points: without stirring; Square points: with stirring.

Figure 3.55 shows the dissolution kinetics curve of this sample. That means that when the film thickness reaches a certain point (like 0.5 $\mu$m), the samples can be well protected by the polymeric film. The protective behavior of a coating comes from two aspects. First, most polymers have limited permeability for water. When Al powder is coated by a polymeric film, it is isolated from NaOH ($Na^+$, $OH^-$), therefore, can not react with NaOH. By this mechanisim, polymer coating slow down the reaction rate. The second aspect, flotation of coated Al powder reduces the contact area and reduces the rate of the reaction. Both of these two aspects were observed during the experiments. From a certain point, they indicate the presence of a polymeric film. The second aspect was quantitatively studied in the previous work in this laboratory where it was shown that approximately 50% of the powder particles float when the average polymer coating thickness is ca. 0.08 nm. In the current study, the smallest film thickness was several nanometers, thus most of the sample powder did float on the solution surface. This effectively prevents solution from surrounding Al powder and reduces the contact area of the sample and the alkali solution.

### 3.6 Solubility of Polymers in Supercritical Carbon Dioxide

Based on the discussion given above that the polymeric films on the surface of Al powder could be not uniform, it could be suggested that the polymer samples are not really completely dissolved in supercritical carbon dioxide. When amount of the polymer loaded in the reactor exceeds its solubility in the available amount of supercritical carbon dioxide, the polymer does not dissolve in carbon dioxide anymore, however, could still form an aerosol at high temperatures. Because the amounts of polymers loaded in the

reactor are very small— 200 mg in 300 $cm^3$, it can be concluded that the solubility of those polymers in supercritical carbon dioxide is smaller than 200 mg in 300 $cm^3$ based on the observation that the polymers were not completely dissolved.

In the literature, there are several methods to measure the solubility of polymers in SC $CO_2$ described. One of the methods is based on the measurements of the cloud formation point in polymeric solutions in SC $CO_2$ using a view cell. The loaded amounts of polymers are large compared to the amounts we used in our studies (0.2 - 0.7 g of polymer per 8 - 16 g of $CO_2$). However, this technique can not applied to our studies because these large amount of polymers are only suitable to those that have large solubility is SC $CO_2$. In other words, the cloud points methods is not sensitive enough to measure the lower solubility of polymers used in our studies. For example, in some publications where this technique was used, it is pointed out that PS, PVF and PMMA (used in our studies) are insoluble in supercritical carbon dioxide at 270 $^{\circ}$ C and 3000 bar (Dimitrov *et al.*, 1998; Rindfleisch *et al.*, 1998). For this reason, a new method suitable for measurements of the solubility of low soluble polymers of this study was developed.

The principle of this new method is simple If the polymer sample in the reactor is dissolved completely, the concentration of the polymer in SC $CO_2$ is proportional to the amount of polymer loaded in the reactor. The increase of the loaded amount of the polymer will increase the concentration. When the solution is saturated by the polymer, further addition of the polymer to the reactor will not increase the concentration in the supercritical phase. In the experiments, tiny amounts of polymer were tried first, then the load amount was increased step by step. At a certain point, the slope of the increase of the measured amount of polymer changed dramatically.

This point was identified as the solubility of this polymer. Concentration of the polymer in SC $CO_2$ affects the average film thickness of polymer—which is further transformed to the concentration of the washed polymer in a solvent. The optical absorbance in the UV region of the organic solutions obtained by washing of the series of polymer coated Al powder samples was measured as a function of the amount of the polymer loaded to the reactor. The absorbance of the solution is proportional to the amount of washed polymer, and, therefore, proportional to the film thickness.

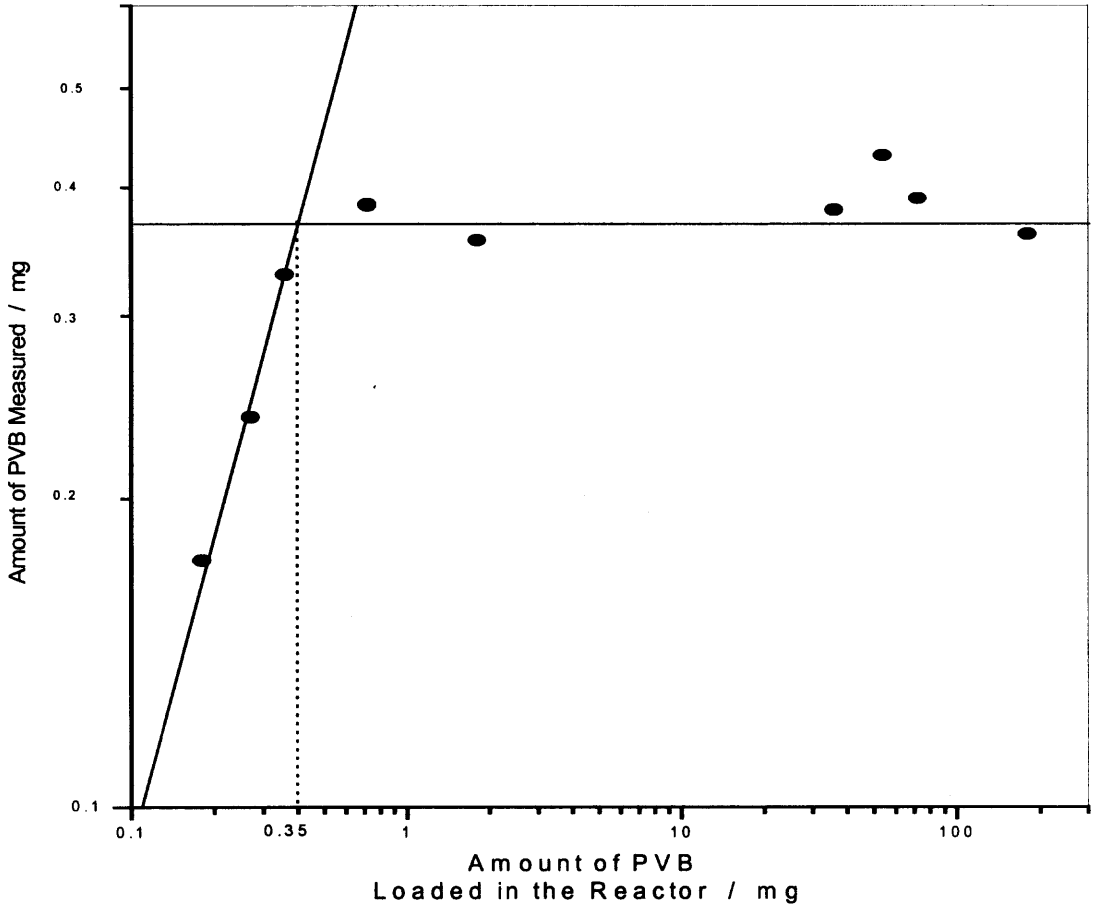


**Figure 3.6** Aluminum powders coated with poly(4-vinyl biphenyl) from SC $CO_2$ at 170 °C and 4100 - 5000 psig. Measurement of solubility of PVB in SC $CO_2$ by means of absorbance in $CH_2Cl_2$

Figure 3.6 illustrates this method applied to determine the solubility of PVB in supercritical carbon dioxide. It shows the dependence of amount of PVB dissolved in 300 ml SC $CO_2$ at 170 °C and 314 atm on the amount of PVB loaded in reactor. It is found that the amount of the dissolved polymer is proportional to the amount of loaded polymer amount until the load amount of 0.35 mg is reached. When the load amount of polymer exceeded 0.35 mg, there measured amount of polymer remain constant. The amount of the polymer is scattered around 0.35mg, so that the solubility of PVB in supercritical carbon dioxide at 170 °C and 314 atm is the point at which the deposited polymer does not increase with the increase of loaded amount polymer, that is 0.35 mg in this case. Since in the current study, the load amounts of polymers were 200 mg, the deposition were made with saturated solution of the polymers.

### 3.7. Morphology of Samples

*Morphology of blank Al powder:* Figure 3.71 shows the ESEM image of the blank Al powder. It shows that the Al powder particles are not exactly spherical, some are elongated and the sizes are not equal.

*Morphology of Al powder coated with PBS in SC $CO_2$* : Al powder was coated with PBS in SC $CO_2$ at 280°C and 5400 psig. The estimated film thickness by UV spectrum was 0.05 $\mu$m. Figure 3.72 presents a ESEM image for this sample. In this image the polymer is also observable as light spheres on the particle's surface.

Figure 3.73 shows the X-ray spectrum for the sample in Figure 3.72. The main peak is at 1.5 keV. This region belongs to Al Ka1, Ka2 and Kb1 emission bands. Although Br La1, La2 and Lb1 bands have almost the same energy values it is doubtful

that they give a contribution in this peak because of the very small amount of the polymer on the powder. Bromine element has a peak at 12 keV, but the limitations of the instrument did not allow to obtain of a the spectrum for energies above 5 keV.

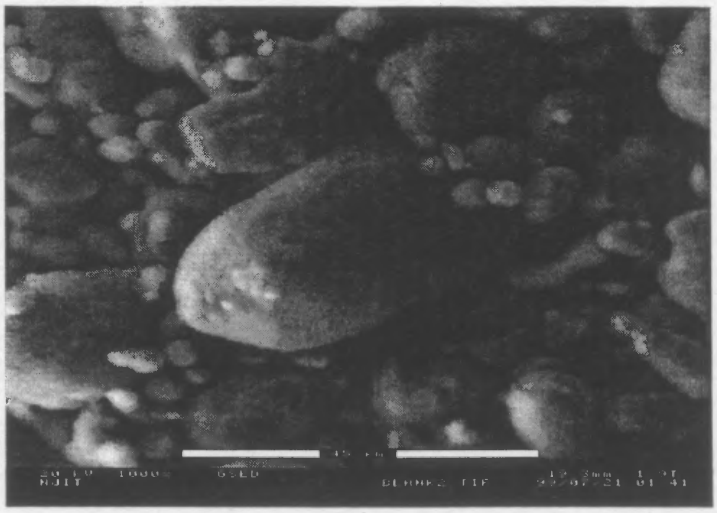

**Figure 3.71** ESEM image of the blank Al powders. Magnifications 750 x.

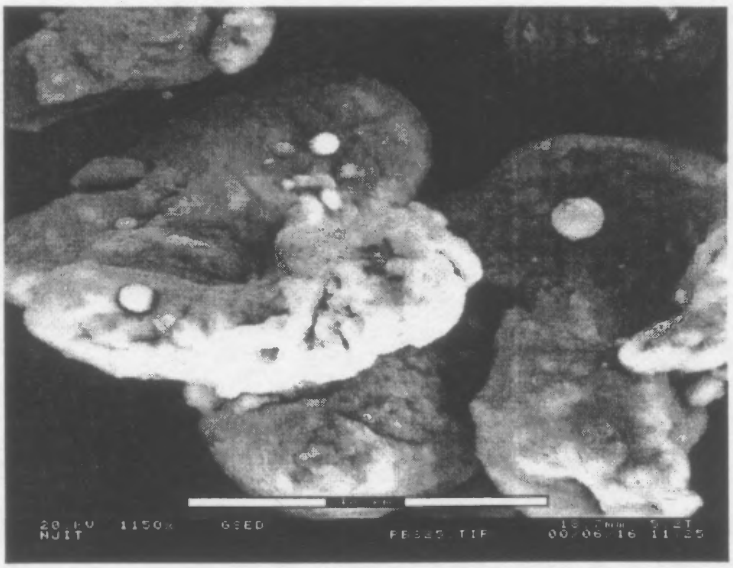

**Figure 3.72** ESEM image of the Al powders coated with PBS in supercritical carbon dioxide at 250 °C and 5000 psig. Magnification 1150x.

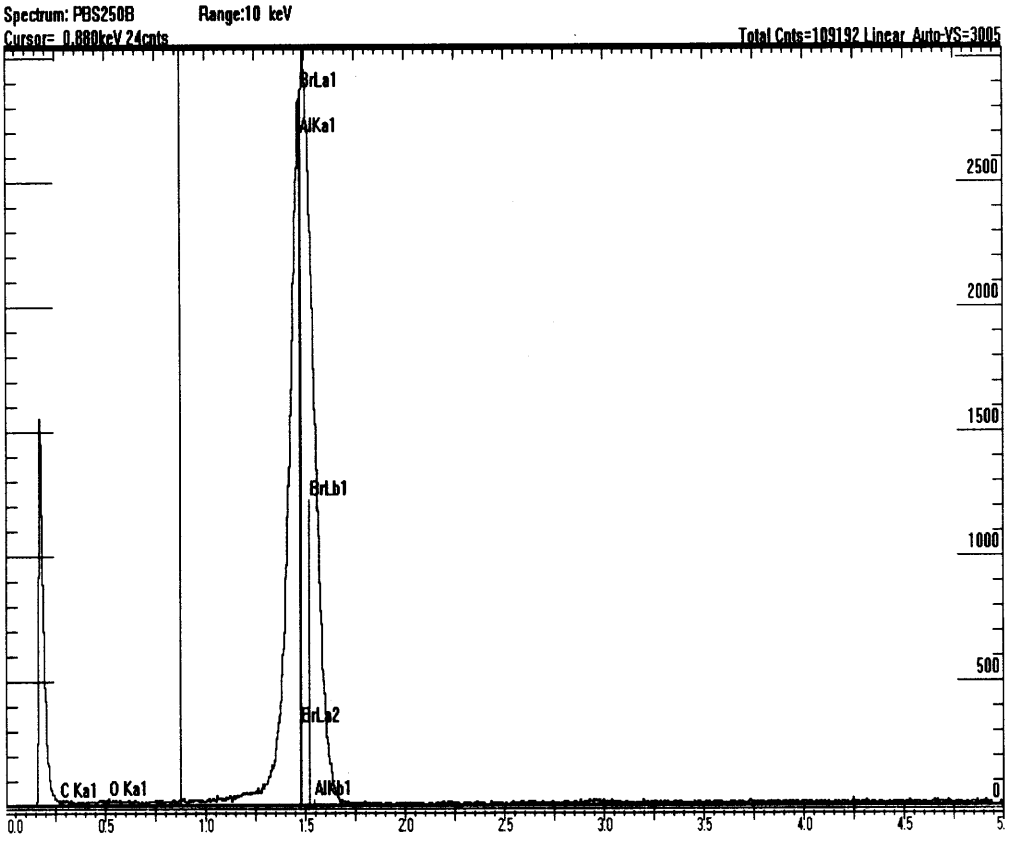


**Figure 3.73** EDX spectrum of Al and Br elements in the same sample in Figure 3.72

*Morphology of Al coated with PBS in $CH_2Cl_2$ with a mole fraction 0.03:* Since polymeric films coated from organic solvents have different protective properties compared to those produced from supercritical carbon dioxide, the ESEM characterization of sample coated from SC $CO_2$ was performed. Figure 3.74 is a ESEM secondary image of a coated Al sample. The magnification was set as 1550x to observe an image of a single particle. It shows that on the surface of the aluminum powder, there is a few smaller particles which could be made from the polymer. Figures 3.75 is the ESEM images of the same sample but the magnification was changed to 500x to observe the general image of the sample. It shows that the surface of the sample is irregular in

shape. No pores or cracks were observed on the surface of the particles. There are some fine particles on the surface or around large Al particles. Comparison of Figures 3.74, 3.75 with figure 3.71 suggests the presence of polymeric particles.

**Figure 3.74** ESEM secondary electron image of a sample coated with PBS in $CH_2Cl_2$ with the polymer mole fraction 0.03. Magnification 1550x.

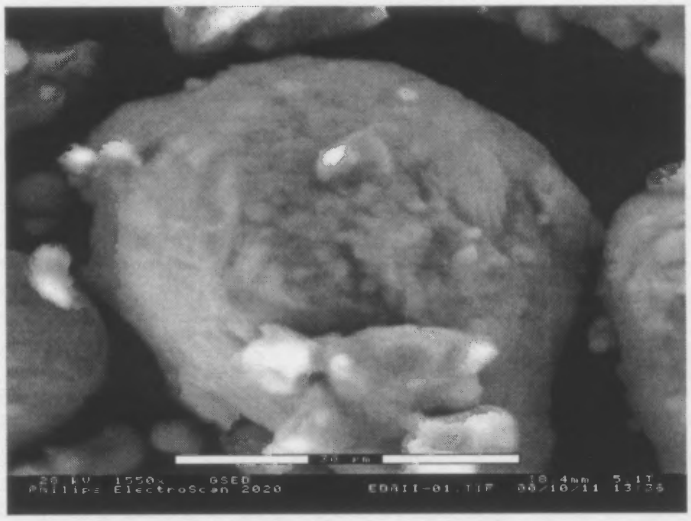

**Figure 3.75** ESEM secondary electron image of a sample coated with PBS in $CH_2Cl_2$ with the polymer mole fraction 0.03. Magnification 1550x.

Figure 3.76 is the Al elemental EDX map which shows the distribution of Al, it looks similar to the sample image. This can be explained that Al element is the dominating element in the sample. This explanation is confirmed by Figure 3.77, which shows the Br element EDX map. The amount of bromine element is not sufficient to produce an image. Compared with Al element, Br is only a small fraction in the sample.

**Figure 3.76** EDX map of Al element in the sample. Corresponds to Figure 3.74.

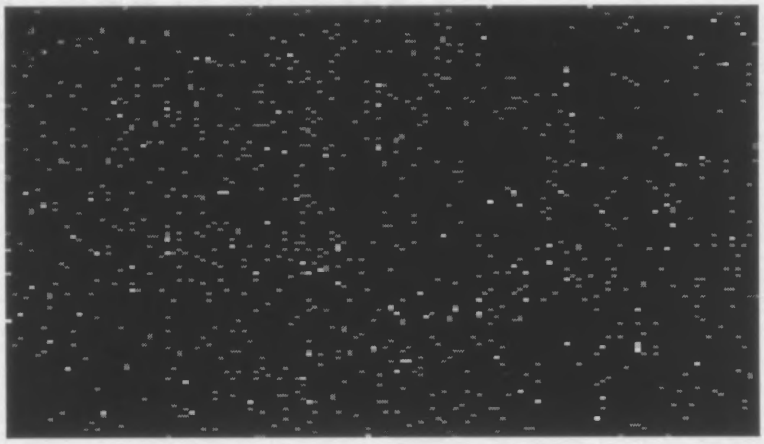

**Figure 3.77** EDX map of Br element in the sample. Corresponds to Figure 3.74.

Figure 3.78 is the EDX spectrum for this sample, there are two gray peaks, one is located close to 1.5 keV, this corresponds to Al element, which has a Ka level emission line at 1.48670 keV, another one is located at 11.65 to 12.2 keV, that is the K level emission line of Br element. The ratio of the peak areas represents the ratio of Al to Br in the sample. The quantitative measurement gave an estimate for the upper limit of atomic ratio of 3:97 for the amount of bromine to aluminum.

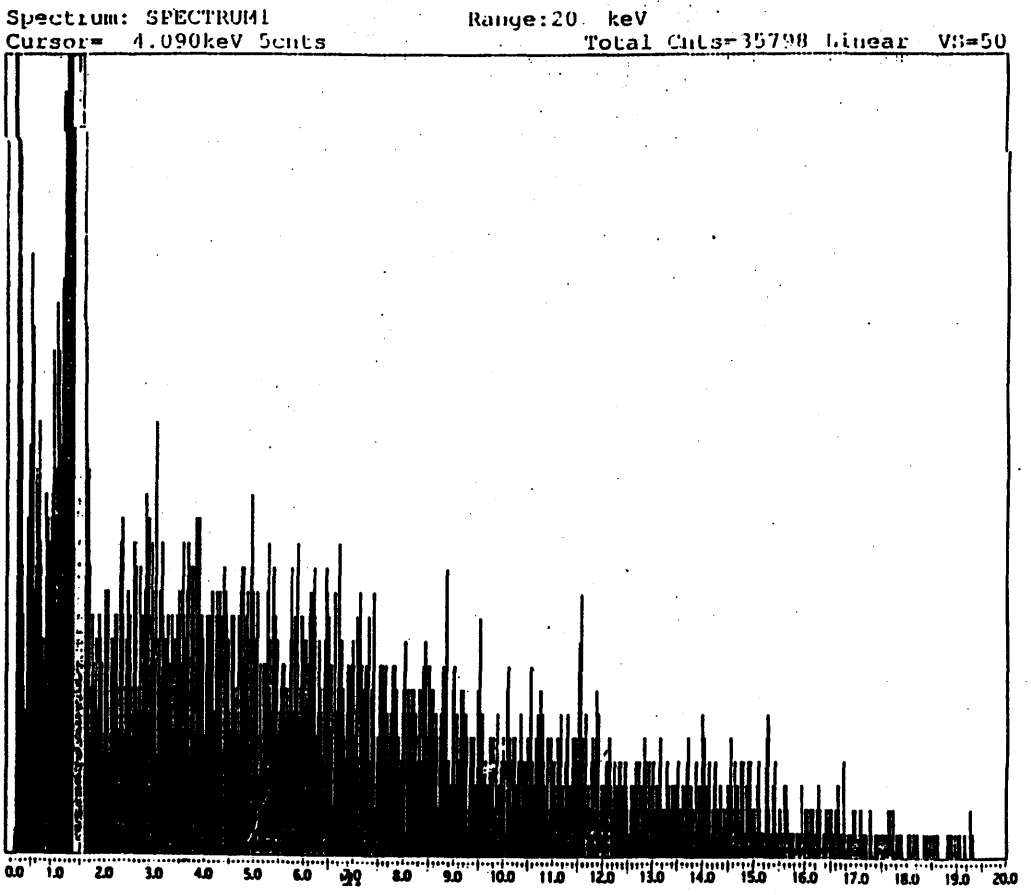


**Figure 3.78** EDX spectrum of the elements in the sample. Corresponds to Fig. 3.74.

**Figure 3.78** EDX spectrum of the elements in the sample. Corresponds to Figure 3.74.

There are some suggestions for the future study of the sample's morphology:

1. To use a traditional high vacuum SEM. Compared with the ESEM used currently, SEM has better resolution and can distinguish Ka line of aluminum element and La line of bromine element;

2. To use magnesium instead of aluminum. Magnesium has a Ka line of 1.25 keV. The larger difference between Ka line of magnesium element and La line of bromine element can allow to distinguish these two lines;

3. To use the highest possible acquisition time for the elemental map — a better map can be obtained in this way. However, longer acquisition time is more expensive, so a compromise time should to be chosen between the consideration of the cost and the precision.

## 3.8 Comparison of Coatings Produced Using Organic Solvents and Supercritical Carbon Dioxide

From the current study, it is apparent that both using organic solvents and SC $CO_2$ for coating have advantages and disadvantages. Using SC $CO_2$ for coating is a promising method. One of the advantages is that carbon dioxide is nontoxic, can be recycled after the use and it is friendly to the environment. Another an advantage is that under supercritical conditions coating can produce very fine particles. Since the film deposited in this way could be very thin, the sample particle size remains almost the same. Another important feature is, the aluminum powder particles coated using carbon dioxide separate from each other, which is important in a number of applications like pyrotechnics formulations, energetic materials, etc.

The disadvantages include that the films on the surface of Al powders could be not smooth enough due to the film roughness and it is difficult to predict the film thickness or the protective properties. Coating in this way can only produce films with a limited film thickness and limited protection. Although temperature, pressure and discharge temperature variation can change the coating condition, an universal result caused by these variations is not established in the current study. Different polymers may have different response following the same condition changes due to the polymer's different physical properties which can be influenced by the change of the conditions. Hence, the optimal condition could not be the same for every polymer, it should be independently determined for each polymer of interest.

Coating process using organic solvents lead to evaporation of organic solvents into air. Because organic substances are difficult to recycle, for large samples, large amount of organic substance is required which results in pollution. The coated samples from common organic solvent are in an aggregate state — the particles "stick" to each other tightly when the targeted film thickness is larger than 20 nm. One additional shortcoming is the time required to produce coating. If the solvent is volatile and only a small amount of a sample is needed, this requires not too much time, usually 40 minutes when the amount of solvent is 10 ml, while large amounts of the sample require larger amounts of a solvent, which requires more time to evaporate. If the solvent used is not volatile, for example, 2-chlorophenol used to dissolve PETP, even if the sample amount is small, it still took several days to totally evaporate.

The advantages of this method include the possibility to predict the film thickness and to obtain almost any desirable film thickness. A better protection of Al powders can be achieved in this way.

# CHAPTER 4

# CONCLUSIONS

In this study, a number of polymeric films were produced on the surface of aluminum powder in supercritical carbon dioxide and from common organic solvents. The protective properties of the polymeric films were characterized quantitatively by the dissolution rate. Compared with the blank aluminum powder, coated particles exhibit an enhanced resistance to the dissolution in aqueous basic solutions from 4 to 13 times and 2 to 5 times for "without stirring" and "with stirring" measurements, respectively. The film thickness was measured using UV spectophotometry. The typical thickness for polymeric films produced in supercritical carbon dioxide is several nanometers. These thin films exhibit a significant protection of aluminum powders from alkali.

The effect of the reactor temperature, pressure and the discharge temperature were investigated for the PVP films. The produced films provide the best protective properties under the reactor temperature of 140 °C, pressure 4000 psig and the discharge temperature of 60 °C. The relationship between the film thickness and the protective properties was not fully established. One possible reason for this is that the films are not uniform. It could be caused by the formation of aerosol during the polymer dissolution in SC $CO_2$ or by the fast deposition of polymer when discharging SC $CO_2$. The optimal conditions for PVP could not be applicable to other polymers, hence, they should be determined for each polymer of interest separately.

The relationship between the film thickness and the dissolution rate constant was established for powders coated from organic solution. The dissolution rate constant decreases sharply with the film thickness when the film thickness is less than 20 nm.

When the film thickness reaches 100 nm, the dissolution rate constant depends weakly on the film thickness. Samples with films of ca. 0.5 μm were produced from organic solvents to investigate the degree of protection and almost complete protection in 120 minutes of dissolution time was achieved.

The morphology of the coated samples was characterized for the blank aluminum powders, the aluminum powders coated with PBS in SC $CO_2$ and the aluminum powders coated with PBS in an organic solution with the polymer mole fraction of 0.03. The EDX spectra were also obtained. The images and the spectra indicate the presence of the polymer on the aluminum powder particles. However, the limitations of the instrument lead to poor elemental image.

A method to measure the solubility of low soluble polymers in supercritical carbon dioxide was developed. The solubility of PVB in SC $CO_2$ was determined. The solubility for PVB is 11.7 mg/L at temperature 170 $^{o}$C and pressure 314 atm.

## REFERENCES


1. Rindfleisch, A.; Diaoia, T. P.; Mchugh. M. A. J. *Phys. Chem.*, **1996**, *100*, 15581-15587.

2. Kim, S.; Johnston, K. P. *ACS Symp, Ser.*, **1987**, *329*, 42.

3. Savage, P. E.; Gopalane,S.; Mizan, T. I.; Martino, C. J.; Brock, E. E. *AIChE Journal*, **1995**, *41*, 1723.

4. Teja, A. S.; Eckert, C. A. *Ind. Eng. Chem. Res.*, **2000**, *39*, 4442-4444.

5. Perrut, M. *Ind. Eng. Chem. Res.*, **2000**, *39*, 12, 4531-4535, 2000.

6. Engelhardt, H. L.; Jurs, P. C. *J.Chem. Inf. Comput. Sci.*, **1997**, *37*, 487-484.

7. Cooper, A. I. *J. Mater. Chem,*. **2000**, *10*, 207.

8. Cooper, A. I.; DeSimone, J. M. *Curr. Opin. Solid State Mater. Sci.*, **1996**, *1*, 761.

9. Ikushima,Y.; Saito, N. *J. Phys. Chem.*, **1992**, *96*, 2293-2297.

10. Hannay, J. B.; Hogarth, J. *Poc. Roy. Soc. London*, **1879**, *29*, 324.

11. Paulaitis, M. E.; Krukonis, V. J.; Kurnik, R. T.; Reid, R. C. *Rev. Chem. Eng.*, **1983**, *1*, 179.

12. McHuge, M. E.; Krukonis, V. *Supercritical Fluid Extraction*; Butterworth: Boston, 1986.

13. Larson, K. A.; King, M. L. *Biotechnol.Prog.*, **1986**, *2*, 73.

14. Ma, X.; Tomasko, D. L. *Ind. Eng. Chem. Res.*, **1997**, *36*, 1586.

15. Petersen, R. C.; Matson, D. W.; Smith, R. D. *J. Amer. Chem. Soc.*, **1986**, *108*, 2100.

16. Matson, D. W.;Fulton, J. L.; Peterson, R. C.; Smith, R. D. *Ind. Eng. Chem. Res.*, **1987**, *26*, 2298.

17. Mohamed, R. S.; Debenedetti, P. G.; Prud'homme, R. K. *AIChE J.*, **1989**, *35*, 325.

16. Matson, D. W.;Fulton, J. L.; Peterson, R. C.; Smith, R. D. *Ind. Eng. Chem. Res.*, **1987**, *26*, 2298.

17. Mohamed, R. S.; Debenedetti, P. G.; Prud'homme, R. K. *AIChE J.*, **1989**, *35*, 325.

18. Chang, C. J.; Randolph, A. D. *AIChE. J.*,**1989**, *35*, 1986.

19. Tom C. J.; Debenedetti, P. G. *Biotechnol. Prog.*, **1991**, *7*, 403.

20. Noriyuki, E. A.; Hirosue, Y. H.; Nakamura, H. *Powder Technology*, **1998**, *97*, 85- 90.

21. Re, M.I.; Biscans, B. *Powder Technology*, **1999**, *101*, 120-133.

22. Perrut, M. *Ind. Eng. Chem. Res.*, **2000**, *39*, 12, 4531-4535, 2000.

23. Tikhonov. V.N. *Analytical Chemistry of Aluminum*; John Wiley & Sons: New York, 1973.

24. Angus, S.; Armstrong, B.; Dereuck K. M. *International Thermaldynamic Tables of the Fluid State Carbon Dioxide;* Pergamon Press: Oxford, 1976.

25. Durrant, P. J.; Durrant, B. *Introduction to Advanced Inorganic Chemistry*; John Wiley & Sons: New York, 1962.

26. Thornton, P. R. *Scanning Electron Microscopy*; Chapman and Hall Ltd.: London, 1968.

27. Wells, O.C.; Boyde, A.; Lifshin, E.; Rezanowich. A. *Scanning Electron Microscopy*; Mcgraw-Hill Book Company: New York, 1974.

28. Hayat, M. A.; Principles and Techniques of Scanning Electron microscopy, vol. 1. Van Nostrand Reinhold Company: New York, 1974.

29. Yamini, Y.; Bahramifa, N. *J. Chem. Eng. Data*, **2000**, *45*, 1, 53-56.

30. Kramer, A.; Thodos, G. *J.Chem. Eng. Data*, **1989**, *34*, 184-187.

31. Bratle, K. D.; Clifford, A. A.; Jafar, S. A.; Shilstone, G. F. *J.Phys. Chem. Ref. Data*, **1991**, *20*, 713.

32. McHugh, M. A.; Paulaitis. M. E. *J. Chem. Data*, **1980**, *25*, 326-329.

33. Zhao, S.; Wang, R.; Yang, G. *The Journal of Supercritical Fluids*, **1995**, *8*, 15-19.

34. Dimitrov, K.; Boyadziev, L.; Tufeu, R.; Cansell, F.; Barth, D. *Journal of Supercritical Fluids,* **1998,** *14*, 41-47.

35. Rindfleisch, F.; Dinoia, T. P.; McHugh, M. A. *J. Phys. Chem.*, **1999,** *100*, 15581-15587.

36. McHugh, M. A.; Krukonis, V. J. *Supercritical Fluid Extraction: Principle and Practice;* Butterworths: Boston, 1986.